Itaconate is an anti-inflammatory metabolite that activates Nrf2 via alkylation of KEAP1

Mills, Evanna L.; Ryan, Dylan G.; Prag, Hiran A.; Dikovskaya, Dina; Menon, Deepthi; Zaslona, Zbigniew

Published in:
Nature

DOI:
10.1038/nature25986

Publication date:
2018

Document Version
Peer reviewed version

Mills, E. L., Ryan, D. G., Prag, H. A., Dikovskaya, D., Menon, D., Zaslona, Z., ... O'Neill, L. A. (2018). Itaconate is an anti-inflammatory metabolite that activates Nrf2 via alkylation of KEAP1. **Nature**. DOI: 10.1038/nature25986

Itaconate is an anti-inflammatory metabolite that activates Nrf2 via alkylation of Keap1

Evanna L. Mills*[1,2,3,4], Dylan G. Ryan*[1], Hiran A. Prag[5], Dina Dikovskaya[6], Deepthi Menon[1], Zbigniew Zaslona[1], Mark P. Jedrychowski[2,3], Ana S. H. Costa[7], Maureen Higgins[6], Emily Hams[8], John Szpyt[3], Marah C. Runtsch[1], Martin S. King[5], Joanna F. McGouran[9], Roman Fischer[10], Benedikt M Kessler[10], Anne F. McGettrick[1], Mark M. Hughes[1], Richard G. Carroll[1, 4], Lee M. Booty[4,5], Elena V. Knatko[6], Paul J. Meakin[11], Michael L.J. Ashford[11], Louise K. Modis[4], Gino Brunori[12], Daniel C. Sévin[13], Padraic G. Fallon[8], Stuart T. Caldwell[14], Edmund R. S. Kunji[5], Edward T. Chouchani[2,3], Christian Frezza[7], Albena T. Dinkova-Kostova[6, 15], Richard C. Hartley[14], Michael P. Murphy[5^], Luke A. O'Neill[1, 4^]

[1]School of Biochemistry and Immunology, Trinity Biomedical Sciences Institute, Trinity College Dublin, Ireland

[2]Department of Cancer Biology, Dana-Farber Cancer Institute, Harvard Medical School, Boston, Massachusetts 02115, USA

[3]Department of Cell Biology, Harvard Medical School, Boston, Massachusetts 02115, USA

[4]GlaxoSmithKline, Gunnels Wood Road, Stevenage, Hertfordshire, UK

[5]MRC Mitochondrial Biology Unit, University of Cambridge CB2 0XY, UK

[6]Jacqui Wood Cancer Centre, Division of Cancer Research, School of Medicine, University of Dundee, Dundee, DD1 9SY Scotland, UK

[7]MRC Cancer Unit, University of Cambridge, Hutchison/MRC Research Centre, Box 197, Cambridge Biomedical Campus, Cambridge, CB2 0XZ, UK

[8]School of Medicine, Trinity Biomedical Sciences Institute, Trinity College Dublin, Ireland

[9]School of Chemistry, Trinity Biomedical Sciences Institute, Trinity College Dublin, Ireland

[10]Nuffield Department of Medicine, Target Discovery Institute, University of Oxford, OX3 7FZ, UK

[11]Division of Molecular and Clinical Medicine, School of Medicine, University of Dundee, Dundee, DD1 9SY Scotland, UK

[12]GlaxoSmithKline, Park Road, Ware, Hertfordshire, UK

[13]Cellzome, GlaxoSmithKline R&D, Heidelberg, Germany

[14]WestCHEM School of Chemistry, University of Glasgow, Glasgow G12 8QQ, UK

[15]Department of Pharmacology and Molecular Sciences, Johns Hopkins University School of Medicine, Baltimore, MD 21205, USA

*These authors contributed equally to this work

^These authors jointly supervised this work

The endogenous metabolite itaconate has recently emerged as a regulator of macrophage function but the precise mechanism of action remains poorly understood[1-3]. We report that itaconate is required for the activation of the antiinflammatory transcription factor nuclear factor-erythroid 2 p45-related factor 2 (Nrf2) by LPS. We find that itaconate directly modifies proteins via alkylation of cysteine residues. Itaconate alkylates cysteines 151, 257, 288, 273 and 297 on Kelch-Like ECH-Associated Protein 1 (Keap1) enabling Nrf2 to increase expression of down-stream genes with anti-oxidant and anti-inflammatory capacity. The activation of Nrf2 is required for the anti-inflammatory action of itaconate. We describe the use of a new cell-permeable itaconate derivative, 4octyl itaconate (OI), which is protective against LPS-induced lethality *in vivo* and decreases cytokine production. We show that type I interferons (IFN) boost immunoresponsive gene 1 (*Irg1*) expression and itaconate production. Furthermore, we find that itaconate production limits the type I IFN response indicating a negative feedback loop involving IFNs and itaconate. Our findings demonstrate that itaconate is a critical anti-inflammatory metabolite acting via Nrf2 to limit inflammation and modulate type I IFNs.

Macrophages have a key role in innate immunity. They respond rapidly to pathogens and subsequently promote an anti-inflammatory phenotype to limit damage and promote tissue repair. The factors driving these changes are incompletely understood. Itaconate, a metabolite synthesized by the enzyme encoded by *Irg1*[1], is elevated in LPS-activated macrophages[2] and has been suggested to limit inflammation by inhibiting succinate dehydrogenase (SDH), a critical proinflammatory regulator[4], however, the details remain unclear.

Itaconate was the most abundant metabolite in LPS-treated human macrophages (Fig. 1a) and reached 5 mM in murine bone marrow-derived macrophages (BMDMs) following LPS stimulation (Fig. 1b, c). Itaconate can disrupt SDH activity, but is less potent than the classic SDH inhibitor malonate (Extended Data Fig. 1), suggesting that it may exert its anti-inflammatory effects via additional mechanisms.

Itaconate contains an electrophilic α,β-unsaturated carboxylic acid that could potentially alkylate protein cysteine residues by a Michael addition to form a 2,3dicarboxypropyl adduct. An attractive candidate protein that undergoes cysteine alkylation is Keap1, a central player in the anti-oxidant response (Fig. 1d). Keap1 normally associates with and promotes the degradation of Nrf2, however alkylation of critical Keap1 cysteines allows newly synthesized Nrf2 to accumulate, migrate to the nucleus and activate a transcriptional antioxidant and anti-inflammatory programme[5]. We therefore examined Keap1/Nrf2 as a target of itaconate.

The cell-permeable itaconate derivative, dimethyl itaconate (DMI)[3] boosted levels of Nrf2 protein, expression of downstream target genes, including hemeoxygenase (Hmox)1, and glutathione (GSH) (Extended Data Fig. 2a-d). However, the lack of a negative charge on the conjugated ester group in DMI increases its reactivity towards Michael addition, making it a far superior Nrf2 activator than itaconate akin to the potent Nrf2 activator dimethylfumarate (DMF)[6]. DMI is rapidly degraded within cells without releasing itaconate[7], hence is unlikely to mimic

endogenous itaconate. Even so, these data indicate that Nrf2 activation is antiinflammatory (Extended Data Fig. 2e, f)[8].

To overcome the limitations of DMI, we synthesised 4-octyl itaconate (OI), a cell-permeable itaconate derivative (Extended Data Fig. 3a). Itaconate and OI had similar thiol reactivity that was far lower than that of DMI (Extended Data Fig. 3b, c, g), making it a suitable cell-permeable itaconate surrogate. Furthermore, OI was hydrolysed to itaconate by esterases in C2C12 cells (Extended Data Fig. 3d) and LPS-activated macrophages (Extended Data Fig. 3e). OI boosted Nrf2 levels (Fig 1e, compare lane 5 to lane 1) and enhanced LPS-induced Nrf2 stabilisation (Fig. 1e, compare lane 6 to lane 2), increasing expression of down-stream target genes[9], including the anti-inflammatory protein Hmox1[10] (Fig. 1f, g). We used a quantitative NAD(P)H:quinone oxidoreductase-1 (NQO1) inducer bioassay[11,12], to assess potency of Nrf2 activation by the CD value (Concentration which Doubles the specific enzyme activity) for NQO1, the prototypical Nrf2 target gene. OI (CD = 2 μM), was more potent than the clinically used Nrf2 activator DMF (CD = 6.5 μM) (Fig. 1h, Extended Data Fig. 3g). OI stimulated GSH (a key anti-oxidant) synthesis (Extended Data Fig. 3g- i). OI also boosted canonical activation of Nrf2 by the pro-oxidant hydrogen peroxide (H_2O_2) (Extended Data Fig. 3j, k). Importantly, 4-octyl 2-methylsuccinate (OMS) and octyl succinate (OS), related octyl esters, which are not Michael acceptors, had no effect on Nrf2 activity confirming the requirement for the itaconate moiety (Extended Data Fig. 3l). Dimethyl malonate (DMM), a potent SDH inhibitor[4], did not activate Nrf2 (Extended Data Fig. 3m), confirming that Nrf2 activation by OI is independent of SDH inhibition.

Itaconate is generated by Irg1 in the mitochondrial matrix and must cross the mitochondrial inner membrane (MIM) to act on Nrf2 in the cytosol. Itaconate is structurally similar to malate, which is transported across the MIM by the dicarboxylate (DIC), citrate (CTP) and oxoglutarate (OGC) carriers. All three carriers transported itaconate, whereas other tested carriers could not (Fig. 2a and Extended Data Fig. 4) suggesting that LPS-induced itaconate is generated in the mitochondrial matrix and is then exported to the cytosol to activate Nrf2.

Our hypothesis is that itaconate activates Nrf2 by alkylation of Keap1 cysteine residue(s)[13-15] akin to the modification of cysteines by fumarate (Extended Data Fig. 5a). Cysteine 151 (Cys151) is a principal sensor on Keap1 for sulforaphane (SFN)[16] and DMF[17]. OI stabilized Nrf2-V5 in COS1 cells co-expressing wild-type Keap1 but not a Cys151S mutant, similarly to SFN (Fig. 2b, compare lanes 16 and 17 to lanes 18 and 19). To analyse Keap1 alkylation directly, we overexpressed FLAG-tagged Keap1 in HEK293T cells and treated with OI. Tandem mass spectrometry (MS) of immunoprecipitated Keap1 revealed that for the Keap1 peptide (144-152), which contains Cys 151, OI treatment increased its mass by 242.15 Da, consistent with alkylation by OI (Fig. 2c). OI also modified other known Keap1 regulatory cysteine residues (Cys257, Cys288 and Cys273) (Extended Data Fig.5b-d, Extended Data Table 1a). Furthermore, itaconate-cysteine adducts, derived in part from glucose and glutamine (Fig. 2d and Extended Data Fig. 6), were detected in LPS-treated macrophages. These data suggest that itaconate activates Nrf2 by alkylating Keap1 cysteines. We further explored cysteine alkylation induced by itaconate using an untargeted MS approach in macrophages treated with OI, or with LPS which elevates

itaconate levels. We identified a number of proteins containing alkylated cysteine residues (Extended Data Table 1b, c). Notably Ldha, which has a critical role in the regulation of glycolysis, was alkylated in OI- and LPS-treated macrophages (Fig. 2e and Extended Data Fig. 5e, f). This modification, here defined as 2,3dicarboxypropylation, generates a stable thioether. As there are no known pathways of removal of such PTMs modified proteins are likely degraded, suggesting this modification will have profound effects on macrophage function.

We next assessed whether itaconate activation of Nrf2 could be antiinflammatory. OI, used at concentrations which did not affect cellular viability, decreased LPS-induced IL-1β mRNA, pro-IL-1β and HIF-1α protein levels, extracellular acidification rate (ECAR) and IL-10 yet had no effect on NFκB activity or TNF-α (Fig. 3a, b and Extended Data Fig. 7a-f). OI also decreased IL-1β mRNA in BMDMs treated with the TLR2 and TLR3 ligands, Pam3CSK and poly I:C, respectively (Extended Data Fig. 7g). LPS-induced ROS, nitric oxide (NO) and iNOS levels were limited by OI (Fig. 3c, d and Extended Data Fig. 7h, i). These effects are likely to be a consequence of ROS detoxification following Nrf2 induction by OI. IL-1β and TNF-α were decreased by OI in human PBMCs (Fig. 3e, Extended Data Fig. 7j). OI also counteracted the pro-inflammatory response to LPS *in vivo.* OI, which activated Nrf2 (Extended Data Fig. 7k), prolonged survival, decreased clinical score and improved body temperature regulation, and decreased IL-1β and TNF-α levels but not IL-10 in an LPS lethality model (Fig. 3f, g and Extended Data Fig. 8f).

OI induction of Hmox1 was blocked in Nrf2-deficient macrophages (Fig. 3h (compare lanes 2, 3 to lanes 8, 9) and Extended Data Fig. 8f) or when Nrf2 was silenced (Extended Data Fig. 8a, d (compare lanes 7, 8 to lanes 11, 12)). Without Nrf2, the decrease in LPS-induced IL-1β with OI was significantly impaired (Fig. 3h (compare lane 6 to lane 12), Extended Data Fig. 8f and 8b-e (compare lanes 6 and 8 to 10 and 12)). Furthermore, two Nrf2 activators, diethyl maleate (DEM) and 15deoxy-Δ12,14-prostaglandin J2 (J2) decreased LPS-induced IL-1β, IL-10, Nos2 and NO (Extended Data Fig. 8g-k). Thus, itaconate activates an anti-inflammatory programme through Nrf2.

We next investigated how switching from a pro- to an anti-inflammatory state might affect itaconate production from aconitate by Irg1. By modelling gene networks controlling *Irg1* expression, Tallam and colleagues (2016) identified IFN response factor (Irf1) as a regulator[18]. Here we show that itaconate levels are increased following IFN-β treatment (Fig. 4a), in agreement with others[19]. Levels of citrate and aconitate, the substrate for Irg1, were reduced by IFN-β as was the downstream metabolite α-ketoglutarate (α-KG) (Extended Data Fig. 9a). These data are consistent with an increase in aconitate conversion to itaconate rather than α-KG. IFN-β enhanced basal and LPS-induced *Irg1* expression (Fig. 4b). LPS and poly I:Cinduced *Irg1* expression in BMDMs lacking type I IFN receptor was decreased (Fig. 4c), indicating that autocrine IFN facilitates Irg1 induction. OI limited the IFN response, decreasing IFN-β and IFN-stimulated gene (ISG)20 expression and Ikappa-B kinase (IKK)-ε and ISG15 protein, IFN-β production in poly I:C-treated PBMCs and LPS-induced IFN-β production *in vivo* (Fig. 4d-g and Extended Data Fig. 9b, c). IFN-β enhanced IL-10 mRNA and protein

expression ± LPS (Extended Data Fig. 9d), suggesting that the decrease in IL-10 following OI treatment is due to reduced type I IFN production [20]. Nrf2 knock-out or knockdown attenuated the reduction of ISG20 expression by OI while the Nrf2 activators, DEM and J2, reduced ISG20 expression (Extended Data Fig. 9e-g). This agrees with increased expression of IRF3-regulated genes in LPS-treated Nrf2-deficient mice[21].

These data suggest the operation a negative feedback loop: itaconate is generated in response to LPS, in part through type I IFNs, and promotes an antiinflammatory programme by Nrf2 activation (Fig. 4h), as well as SDH inhibition[3,22]. This limits further inflammatory gene expression and its own production by downregulating the IFN response. This helps explain why Nrf2-deficient mice are more sensitive to septic shock[21], even though under certain circumstances these mice are protected from inflammation[23]. Our identification of itaconate as an inflammatory regulator, that directly modifies proteins through a newly identified post-translational modification, unveils therapeutic opportunities to use itaconate or OI to treat inflammatory diseases[24]. Most recently Shen and colleagues (2017) have made an intriguing link from itaconate to Vitamin B12 which warrants further investigation in the context of inflammation and immunity[25]. Further understanding the role of itaconate as an anti-inflammatory metabolite and regulator of type I IFNs is likely to yield new insights into the pathogenesis of inflammatory diseases.

Author Contributions

E. L. Mills and D. G. Ryan designed and performed experiments and analysed the data. E. L. Mills wrote the manuscript with assistance from all other authors. D. Menon, M. M. Hughes, M. C. Runtsch and A. F. McGettrick performed in vitro experiments using OI. R. G. Carroll, D. Sevin, A. S. H. Costa and C. Frezza assisted with the metabolomics analysis. Z. Zaslona, P. G. Fallon and E. Hams assisted with the *in vivo* mouse LPS trials. S. T. Caldwell and R. C. Hartley were responsible for the design and synthesis of octyl esters. H. A. Prag, E. R. S. Kunji, M. S. King, and L. M. Booty assessed the effect of OI and itaconate on mitochondrial parameters and itaconate transport. D. Dikovskaya, M. Higgins and A. T. Dinkova-Kostova performed the Nqo1 assay and Keap1 WT and Cys151S mutant experiments. J. F. McGouran, R. Fisher, B. M. Kessler, E. T. Chouchani, M. P. Jedrychowski, J. Szpyt assisted with mass spectrometry experiments. L. Modis and G. Bruori provided guidance and advice. E. V. Knatko, P. J. Meakin, M. L. J. Ashford assisted with experiments in Nrf2-deficient mice. L. A. O'Neill conceived ideas and oversaw the research programme. M. P. Murphy provided advice, reagents and oversaw a portion of the work.

Author Information

Reprints and permissions information is available at www.nature.com/reprints. The authors declare no competing financial interests. Correspondence and requests for materials should be addressed to L. A. O'Neill. (laoneill@tcd.ie)

Acknowledgements

We thank Michael McMahon and John D. Hayes (University of Dundee) for plasmids, and Cancer Research UK (C20953/A18644) and the BBSRC (BB/L01923X/1) for financial support for ATDK. This work was supported by a Wellcome Trust Investigator award to RCH (110158/Z/15/Z), a grant to MPM from the Medical Research Council UK (MC_U105663142), a Wellcome Trust Investigator award to MPM (110159/Z/15/Z), and a grant to ERSK and MSK from the Medical Research Council UK (MC_U105663139). BMK and RF are supported by the Kennedy Trust Fund. We acknowledge Metabolon for their assistance with the metabolic work and analysis. The O'Neill lab acknowledges the following grant support: European Research Council (ECFP7-ERC-MICROINNATE), Science Foundation Ireland Investigator Award (SFI 12/IA/1531), GlaxoSmithKline Visiting Scientist Programme and The Wellcome Trust (oneill-wellcometrust-metabolic, grant number 205455). ETC is supported by the Claudia Adams Barr Program.

References

1 Michelucci, A. *et al.* Immune-responsive gene 1 protein links metabolism to immunity by catalyzing itaconic acid production. *Proc Natl Acad Sci U S A* **110**, 7820-7825, doi:10.1073/pnas.1218599110 (2013).

2 Strelko, C. L. *et al.* Itaconic acid is a mammalian metabolite induced during macrophage activation. *J Am Chem Soc* **133**, 16386-16389, doi:10.1021/ja2070889 (2011).

3 Lampropoulou, V. *et al.* Itaconate Links Inhibition of Succinate Dehydrogenase with Macrophage Metabolic Remodeling and Regulation of Inflammation. *Cell Metab* **24**, 158-166, doi:10.1016/j.cmet.2016.06.004 (2016).

4 Mills, E. L. *et al.* Succinate Dehydrogenase Supports Metabolic Repurposing of Mitochondria to Drive Inflammatory Macrophages. *Cell* **167**, 457-470 e413, doi:10.1016/j.cell.2016.08.064 (2016).

5 Hayes, J. D. & Dinkova-Kostova, A. T. The Nrf2 regulatory network provides an interface between redox and intermediary metabolism. *Trends in biochemical sciences* **39**, 199-218, doi:10.1016/j.tibs.2014.02.002 (2014).

6 Brennan, M. S. *et al.* Dimethyl fumarate and monoethyl fumarate exhibit differential effects on KEAP1, NRF2 activation, and glutathione depletion in vitro. *PLoS One* **10**, e0120254, doi:10.1371/journal.pone.0120254 (2015).

7 ElAzzouny, M. *et al.* Dimethyl Itaconate Is Not Metabolized into Itaconate Intracellularly. *J Biol Chem* **292**, 4766-4769, doi:10.1074/jbc.C117.775270 (2017).

8 Kobayashi, E. H. *et al.* Nrf2 suppresses macrophage inflammatory response by blocking proinflammatory cytokine transcription. *Nat Commun* **7**, 11624, doi:10.1038/ncomms11624 (2016).

9 Lee, J. M., Calkins, M. J., Chan, K., Kan, Y. W. & Johnson, J. A. Identification of the NF-E2-related factor-2-dependent genes conferring protection against

oxidative stress in primary cortical astrocytes using oligonucleotide microarray analysis. *J Biol Chem* **278**, 12029-12038, doi:10.1074/jbc.M211558200 (2003).

10 Piantadosi, C. A. *et al.* Heme oxygenase-1 couples activation of mitochondrial biogenesis to anti-inflammatory cytokine expression. *The Journal of biological chemistry* **286**, 16374-16385, doi:10.1074/jbc.M110.207738 (2011).

11 Prochaska, H. J. & Santamaria, A. B. Direct measurement of NAD(P)H:quinone reductase from cells cultured in microtiter wells: a screening assay for anticarcinogenic enzyme inducers. *Analytical biochemistry* **169**, 328-336 (1988).

12 Fahey, J. W., Dinkova-Kostova, A. T., Stephenson, K. K. & Talalay, P. The "Prochaska" microtiter plate bioassay for inducers of NQO1. *Methods in enzymology* **382**, 243-258 (2004).

13 Dinkova-Kostova, A. T. *et al.* Direct evidence that sulfhydryl groups of Keap1 are the sensors regulating induction of phase 2 enzymes that protect against carcinogens and oxidants. *Proc Natl Acad Sci U S A* **99**, 11908-11913, doi:10.1073/pnas.172398899 (2002).

14 McMahon, M., Lamont, D. J., Beattie, K. A. & Hayes, J. D. Keap1 perceives stress via three sensors for the endogenous signaling molecules nitric oxide, zinc, and alkenals. *Proc Natl Acad Sci U S A* **107**, 18838-18843, doi:10.1073/pnas.1007387107 (2010).

15 Dinkova-Kostova, A. T., Kostov, R. V. & Canning, P. Keap1, the cysteinebased mammalian intracellular sensor for electrophiles and oxidants. *Arch Biochem Biophys* **617**, 84-93, doi:10.1016/j.abb.2016.08.005 (2017).

16 Zhang, D. D. & Hannink, M. Distinct cysteine residues in Keap1 are required for Keap1-dependent ubiquitination of Nrf2 and for stabilization of Nrf2 by chemopreventive agents and oxidative stress. *Mol Cell Biol* **23**, 8137-8151 (2003).

17 Linker, R. A. *et al.* Fumaric acid esters exert neuroprotective effects in neuroinflammation via activation of the Nrf2 antioxidant pathway. *Brain* **134**, 678-692, doi:10.1093/brain/awq386 (2011).

18 Tallam, A. *et al.* Gene Regulatory Network Inference of Immunoresponsive Gene 1 (IRG1) Identifies Interferon Regulatory Factor 1 (IRF1) as Its Transcriptional Regulator in Mammalian Macrophages. *PLoS One* **11**, e0149050, doi:10.1371/journal.pone.0149050 (2016).

19 Naujoks, J. *et al.* IFNs Modify the Proteome of Legionella-Containing Vacuoles and Restrict Infection Via IRG1-Derived Itaconic Acid. *PLoS Pathog* **12**, e1005408, doi:10.1371/journal.ppat.1005408 (2016).

20 Guarda, G. *et al.* Type I interferon inhibits interleukin-1 production and inflammasome activation. *Immunity* **34**, 213-223, doi:10.1016/j.immuni.2011.02.006 (2011).

21 Thimmulappa, R. K. *et al.* Nrf2 is a critical regulator of the innate immune response and survival during experimental sepsis. *J Clin Invest* **116**, 984-995, doi:10.1172/JCI25790 (2006).

22 Cordes, T. *et al.* Immunoresponsive Gene 1 and Itaconate Inhibit Succinate Dehydrogenase to Modulate Intracellular Succinate Levels. *J Biol Chem* **291**, 14274-14284, doi:10.1074/jbc.M115.685792 (2016).
23 Freigang, S. *et al.* Nrf2 is essential for cholesterol crystal-induced inflammasome activation and exacerbation of atherosclerosis. *Eur J Immunol* **41**, 2040-2051, doi:10.1002/eji.201041316 (2011).
24 Dinarello, C. A. Interleukin-1 in the pathogenesis and treatment of inflammatory diseases. *Blood* **117**, 3720-3732, doi:10.1182/blood-2010-07273417 (2011).
25 Shen, H. *et al.* The Human Knockout Gene CLYBL Connects Itaconate to Vitamin B12. *Cell* **171**, 771-782 e711, doi:10.1016/j.cell.2017.09.051 (2017).

Figure Legends

Figure 1. Itaconate activates Nrf2. a-c LPS-induced itaconate (**a**, *n*=12, 4 h; **b, c** *n*=5, 24 h). Red and blue dots represent metabolites significantly up- or downregulated by LPS, respectively. **d** Reactivity of itaconate with Keap1 thiol group. **e, g** LPS-induced Nrf2 (**e**, 24 h) and Hmox1 (**e**, 6 h) ± OI. **f** Nrf2 target gene expression ± LPS (6 h) ± OI (Nqo1, Gclm, Hmox1 *n*=12; Gsr, 6Pdg, Taldo1 *n*=6). **h** NQO1 activity in Hepa1c1c7 cells treated as indicated (48 h, *n*=8). Data are mean ± s.e.m. *P* values calculated using one-way ANOVA. Blots are representative of 3 independent experiments. In the box plots, line shows mean. For gel source data, see Supplementary Figure 1.

Figure 2. Itaconate alkylates cysteines. a Itaconate transport by the indicated carriers (*n*=4). **b** Nrf2 and Keap1 protein following co-transfection with Nrf2-V5 ± wildtype or Cys151S mutant Keap1. **c** MS/MS spectrum of Cys151-containing Keap1 peptide following OI treatment. **d** Metabolite tracing to itaconate-cysteine adduct ± LPS (24 h, *n*=5). **e** Ldha Cys84 alkylation ± LPS (24 h) or OI (250 µM, 4 h) (*n*=4). Data are mean ± s.e.m or S.D. (in **a**). *P* values calculated using one-way or two-way ANOVA for multiple comparisons or two-tailed student t-test for paired comparisons.
Blots are representative of 3 independent experiments. For gel source data, see Supplementary Figure 1.

Figure 3. OI limits IL-1β in an Nrf2-dependent manner and protects against LPS lethality. a-d LPS (24 h), induced IL-1β mRNA (**a**, *n*=3), IL-1β and HIF-1α protein (**b**), and ROS and NO production (**c, d**, *n*=3, MFI, mean fluorescence intensity) ± OI. **e** IL-1β mRNA in PBMCs treated as in **a-d** (*n*=3). **f** Survival, clinical score and body temperature measurements in mice (*n*=10) injected i.p ± OI (50 mg/kg, 2 h) ± LPS (15 mg/kg). **g** Serum IL-1β and TNF-α from mice i.p. injected ± OI (50 mg/kg, 2 h) ± LPS (2.5 mg/kg, 2 h, *n*=3 vehicle, OI; *n*=15 LPS, OI+LPS). **h** Nrf2, Hmox1 and IL-1β protein in wild-type and Nrf2 KO BMDMs treated with LPS (6 h) ± OI. Data are mean ± s.e.m. *P* values calculated using one-way ANOVA. Blots are representative of 3 independent experiments. For gel source data, see Supplementary Figure 1.

Figure 4. A feedback loop exists between itaconate and IFN-β. a Metabolite levels ± IFN-β (1000 U/ml; 27 h; *n*=5). **b** LPS (24 h)-induced Irg1 expression ± IFN-β (1000 U/ml; *n*=3). **c** Irg1 expression in wild-type (WT) and IFN receptor (IFNR)deficient

BMDMs ± LPS or poly I:C (40 μg/ml) for 24 h (*n*=3). **d** IFN-β (*n*=3) expression ± LPS (24 h) ± OI. **e** ISG15 and IKK-ε ± LPS (24 h) ± OI. **f** IFN-β protein expression in PBMCs ± poly I:C (20 μg/ml; 24 h) ± OI (*n*=3). **g** Serum IFN-β from mice i.p. injected ± OI (50 mg/kg, 2 h) ± LPS (2.5 mg/kg; 2 h) (*n*=3 vehicle, OI; *n*=15 LPS, OI+LPS). **h** The anti-inflammatory role of itaconate. Data are mean ± s.e.m. *P* values calculated using one-way ANOVA. Blots are representative of 3 independent experiments. **f** is representative from one of two human donors. For gel source data, see Supplementary Figure 1.

METHODS

Isolation of Human PBMC

Human PBMC were isolated from human blood using Lymphoprep (Axis-Shield). 30 ml of whole blood was layered on 20 ml lymphoprep and spun for 20 min at 2,000 rpm with no brake on. The PBMCs were isolated from the middle layer. PBMCs were maintained in RPMI supplemented with 10% (vol/vol) FCS, 2 mM L-glutamine, and 1% penicillin/streptomycin solution.

Generation of human macrophages

Blood was layered on Histopaque and centrifuged at 800 x *g* for 20 minutes, acceleration 9, deceleration at 4. The PBMC layer was isolated and the macrophages were sorted using magnetic-activated cell sorting (MACS) CD14 beads Cells were plated at 0.5 x 10^6 cells/ml in media containing M-CSF (100 ng/ml) and maintained at 37°C, 5% CO_2 for 5 days, to allow differentiation into macrophages. For further details see the Supplementary Methods section.

Generation and treatment of bone marrow-derived macrophages (BMDMs) Mice were euthanized in a CO_2 chamber and death was confirmed by cervical dislocation. Bone marrow cells were extracted from the leg bones and differentiated in DMEM (containing 10% foetal calf serum, 1% penicillin streptomycin and 20% L929 supernatant) for 6 days, at which time they were counted and replated for experiments. Unless stated, 5 X 10^6 BMDMs/ml were used in *in vitro* experiments. Unless stated the LPS concentration used was 100 ng/ml, the DMI and OI concentration was 125 μM and in experiments were pre-treatments prior to LPS stimulation this was for 3 h.

Synthesis of Itaconate compounds

For details on synthesis and characterization of chemical compounds details see Supplementary Methods.

Metabolomic analysis with Metabolon

Macrophages were plated at 2x10^6/well in 6-well plates and treated as required BMDMs, *n*=5, human macrophages *n*=12. Analysis was performed by Metabolon. For further details see the Supplementary Methods section.

Metabolite Measurements for absolute succinate and itaconate quantification and metabolite tracing

Cells were treated as desired. For tracing studies, immediately prior to LPS stimulation the media was removed and replaced with DMEM media (1 ml) containing U-^{13}C-glucose (4.5 g/L) or U-^{13}C-glutamine (584 mg/mL) deplete of ^{12}C- glucose or ^{12}C-glutamine. Samples were extracted in methanol/acetonitrile/water, 50:30:20 v/v/v (1 ml per 1x10^6 cells) and agitated for 15 min at 4°C in a Thermomixer and then incubated at -20°C for 1 h. Samples were centrifuged at maximum speed for 10 min at 4°C. The supernatant was transferred into a new tube and centrifuged again at maximum speed for 10 min at 4°C. The supernatant was transferred autosampler vials. LC-MS analysis was performed using a Q Exactive mass spectrometer coupled to a Dionex U3000 UHPLC system (Thermo). For further details see Supplementary Methods.

Western blotting

Protein samples from cultured cells were prepared by direct lysis of cells in 5X Laemmli sample buffer, followed by heating at 95°C for 5 min. For spleen samples, 30 mg of spleen was homogenized in RIPA buffer using the Qiagen TissueLyserII system. The resulting homogenate was centrifuged at 14000 rpm for 10 min at 4°C, and supernatants were used for SDS-PAGE. Protein samples were resolved on 8% or 12% SDS-PAGE gels and were then transferred onto polyvinylidene difluoride (PVDF) membrane using either a wet or semi-dry transfer system. Membranes were blocked in 5% (w/v) dried milk in Tris-buffered saline-Tween (TBST) for at least one hour at room temperature. Membranes were incubated with primary antibody, followed by the appropriate horseradish peroxidase-conjugated secondary antibody. They were developed using LumiGLO enhanced chemiluminescent (ECL) substrate (Cell Signalling). Bands were visualized using the GelDoc system (Biorad).

Real-time PCR

Total RNA was isolated using the RNeasy Plus Mini kit (Qiagen) and quantified using a Nanodrop 2000 UV-visible spectrophotometer. cDNA was prepared using 20–100 ng/µl total RNA by a reverse transcription-polymerase chain reaction (RT-PCR) using a high capacity cDNA reverse transcription kit (Applied Biosystems), according to the manufacturer's instructions. Real-time quantitative PCR (qPCR) was performed on cDNA using SYBR Green probes. qPCR was performed on a 7900 HT Fast RealTime PCR System (Applied Biosystems) using Kapa fast master mix high ROX (Kapa Biosystems, for SYBR probes) or 2X PCR fast master mix (Applied Biosystems, for Taqman probes). For SYBR primer pair sequences see Supplementary Methods. Fold changes in expression were calculated by the Delta Delta Ct method using mouse Rps18 as an endogenous control for mRNA expression. All fold changes are expressed normalized to the untreated control.

NQO1 bioassay

Inducer potency was quantified by use of the NQO1 bioassay in Hepa1c1c7 murine hepatoma cells [11,12]. Cells (10^4 per well of a 96-well plate) were grown for 24 h and

treated (*n*=8) to serial dilutions of compounds for 48 h prior to lysis. NQO1 enzyme activity was quantified in cell lysates using menadione as a substrate. Protein concentrations were determined in aliquots from the same cell lysates by the bicinchoninic acid (BCA) assay (Thermo Scientific). The CD value was used as a measure of inducer potency. For assays examining the effect of GSH on inducer potency, 50 µM of each compound was incubated with 1 mM GSH in the cell culture medium at 37°C for 30 min before treatment.

Preparation of rat liver mitochondria

Female Wistar rats aged between 10 to 12 weeks (Charles River, UK) were culled by stunning and cervical dislocation prior to the liver being excised and stored in icecold buffer (STE buffer (250 mM sucrose, 5 mM Tris-Cl, 1 mM EGTA (pH 7.4 at 4 °C)). Rat liver mitochondria were isolated by homogenisation and differential centrifugation at 4°C in STE buffer[26]. Briefly, minced tissue was homogenised in STE buffer before centrifugation (1, 000 x g, 3 min, 4°C) and centrifuging the resulting supernatant (10, 000 x g, 10 min, 4°C). The mitochondrial pellet was resuspended in fresh STE before centrifuging (10, 000 x g, 10 min, 4°C). The resulting pellet was resuspended in STE and assayed for protein concentration via BCA assay (Thermo Scientific) against a BSA standard curve.

Preparation of bovine heart mitochondrial membranes

Bovine heart mitochondria were isolated by differential centrifugation in 250 mM sucrose, 10 mM Tris-Cl, 0.2 mM EDTA (pH 7.8 at 4°C). To prepare membranes, bovine heart mitochondria were blended with MilliQ water at 4°C before adding KCl to a final concentration of 150 mM and blending until homogenous. The suspension was centrifuged (13, 500 x g, 40 min, 4°C) and the pellet resuspended in resuspension buffer (20 mM Tris-Cl, 1 mM EDTA, 10% glycerol, pH 7.55 at 4°C) before homogenisation and assaying for protein by BCA assay (Thermo Scientific)[27].

Measuring complex II+III activity

Bovine heart mitochondrial membranes (80 µg protein/ml) were incubated in 50 mM potassium phosphate buffer (50 mM potassium phosphate, 1 mM EDTA, pH 7.4, 4°C) supplemented with 3 mM KCN, 4 µM rotenone and succinate. In a 96-well microplate, inhibitor or vehicle control and membrane incubation were plated and incubated for 10 minutes at 30°C. Alternatively, where indicated, itaconate was incubated with membranes and removed by twice centrifuging membranes and resuspending in non-itaconate containing buffer, prior to plating with 1 mM succinate. Oxidised cytochrome-c was added prior to measuring the respiratory chain activity by assessing the reduction of cytochrome-c spectrophotometrically at 550 nm at 20 second intervals for 5 min at 30°C. Final concentrations were 10 µg protein/well bovine heart membranes and 30 µM ferricytochrome c.

Measuring rat liver mitochondrial respiration

Respiration of rat liver mitochondria was assessed with an Oxygraph-2K (OROBOROS instruments high resolution respirometry, Austria). Rat liver mitochondria (0.5 mg mitochondrial protein/ml) were added to KCl buffer (pH 7.2, 37°C) and respiration

assessed in the presence of 4 µg/ml rotenone, 1 mM succinate, 1 µM FCCP and inhibitors or buffer control.

Assessing itaconate ester reactivity with glutathione

1 or 5 mM GSH and 5 mM itaconate esters or vehicle control were incubated in KCl buffer (pH 7.2 or 8) at 37°C for 2 hours, where indicated, 10 µg recombinant glutathione-S-transferase (GST) was added to the incubation. The reaction was stopped by acidification with 5% sulfosalicylic acid prior to assessing glutathione content by the GSH recycling assay as described previously [28].

Itaconate transport assays

Itaconate transport by mitochondrial carriers was assessed as described previously [29]. For further details see the Supplementary Methods section.

Cell uptake of itaconate

C2C12 mouse myoblasts were plated at 300,000 cells/well in a 6-well plate in complete growth medium and adhered overnight in a humidified 5% CO_2, 37°C incubator. The following day, media was replaced with serum free DMEM containing itaconate esters and cells were treated for 30 minutes at 37°C. Cells were extracted as described above (method for succinate quantification), with MS internal standard (100 pmoles) added and stored at -80°C prior to LC-MS/MS analysis. For further details see Supplementary Methods.

LC-MS/MS analysis was performed using an LCMS-8060 mass spectrometer (Shimadzu) with a Nexera X2 UHPLC system (Shimadzu). For further details see Supplementary Methods

Keap1 cysteine target validation

COS1 cells (2.5 x 10^5 per well) in 6-well plates were co-transfected (Lipofectamine 2000) with 0.8 µg of Nrf2-V5 and 1.6 µg of wild-type or Cys151S mutant Keap1[14], or 1.6 µg of pcDNA. Cells were grown for 21 h then treated with 20 or 100 µM OI, 5 µM sulforaphane (SFN) or 0.1% acetonitrile (ACN, vehicle) for 3 h. Cell were washed in PBS and lysed in 200 µl of SDS-lysis buffer [50 mM Tris-HCl pH 6.8, 2% (w/v) sodium dodecyl sulfate (SDS) and 10% (v/v) Glycerol]. Lysates were sonicated (20 sec at 30% amplitude using Vibra-Cell ultrasonic processor, Sonic) and boiled (3 min), DTT and Bromophenol blue were added up to 0.1M and 0.02% (w/v) final concentrations, respectively. Proteins (10 µg) were resolved on a gradient (4-12%) NuPAGE SDS gel, transferred onto nitrocellulose membranes, and immunoblotted with anti-Keap1 (rat monoclonal, Merk Millipore, clone 144), anti-Nrf2 (rabbit monoclonal, CST), and anti-β-actin (mouse monoclonal, Sigma) antibodies. HRP- or IRDye-labelled secondary antibodies were used interchangeably, followed by either ECL-detection or scanning using Odyssey imager (Li-COR).

Enzyme-linked immunosorbent assay (ELISA)

Cytokine concentrations in cell supernatants were measured using enzyme-linked immunosorbent assay (ELISA) Duoset kits for mouse IL-10 and TNF-α and human IFN-β and IL-1β, according to the manufacturer's instructions. Cytokine concentrations in serum samples isolated from whole blood were measured using Quantikine ELISA kits for mouse or human IL-1β, IFN-β IL-10 and TNF-α. Duoset and Quantikine kits were from R&D Systems. Optical density values were measured at a wavelength of 450 nm, using a FLUOstar Optima plate reader (BMG Labtech). Concentrations were calculated using a 4-parameter fit curve.

FACS Analysis of reactive oxygen species (ROS)

BMDMs were seeded at $0.5x10^6$ cells/ml and treated as normal. 2 hours prior to staining, 100% EtOH was added to the dead cell control well. 30 minutes prior to the end of the stimulation, CellROX (5 µM) was added directly into the cell culture medium. Supernatants of cells that were to be stained with Aqua Live/Dead were removed, and an Aqua Live/Dead dilution (1 ml; 1 in 1000 in PBS) was added to each well. Cells were incubated in tinfoil at 37°C for 30 min. Cells were washed with PSB, scraped in PBS (0.5 ml), and transferred to polypropylene FACS tubes. Samples were analyzed using a Dako CyAn flow cytometer, and data was analyzed using FlowJo software. Mean fluorescence intensity (MFI) was quantified as a measure of cellular ROS production.

NO assay

Nitric oxide concentrations in cell supernatants were measured using Greiss reagent assay kit from Thermo Fischer Scientific according to the manufacturer's instructions. Optical density values were measured at a wavelength of 548 nm, using a SoftMax Pro plate reader. Concentrations were calculated using a linear standard curve.

GSH/GSSG measurements

BMDMs were plated at $0.1x10^6$ cells/ml in opaque 96-well plates. Cells were pretreated with OI (125 µM) for 2 h and then stimulated with H_2O_2 (100 µM) for 24h. After 24 h cell media was removed and GSH/GSSG was quantified using MyBio GSH/GSSG-Glo Assay (V6611) as per manufacturer's instructions. Luminescence was quantified using a FLUOstar Optima plate reader.

LDH assay

Cells were plated at $0.5x10^6$ cells/ml in white 24-well plates (500 µl/well) and treated as required. Cytotoxicity, as determined by LDH release, was assayed using CytoTox96 Non-radioactive Cytotoxicity Assay kit (Promega) according to the manufacturer's instructions.

Seahorse analysis of lactate production

Cells were plated at $0.2x10^6$ cells/well of a 24-well Seahorse plate. Cells were treated and stimulated as normal. A utility plate containing calibrant solution (1 ml/well) was placed in a CO_2-free incubator at 37°C overnight. The following day media was removed from cells and replaced with glucose-supplemented XF assay buffer (500

µl/well) was placed in a CO_2-free incubator for at least 0.5 h. Inhibitors (Oligomycin, carbonyl cyanide-*4*-(trifluoromethoxy)phenylhydrazone (FCCP), 2DG, Rotenone; 70 µl) were added to the appropriate port of the injector plate. This plate together with the utility plate was run on the Seahorse for calibration. Once complete, the utility plate was replaced with the cell culture plate and run on the Seahorse XF-24.

Endotoxin-induced model of sepsis

For cytokine measurements mice were treated intraperitoneally (i.p.) ± OI (50 mg/kg) in 40% cyclodextrin in PBS or vehicle control for 2 h prior to stimulation with LPS (Sigma; 2.5 mg/kg) i.p. for 2 h. Mice were euthanized in a CO_2 chamber, blood samples were collected and serum was isolated. Cytokines were measured using R&D ELISA kits according to manufactures protocol. For temperature recording mice (n=10 per group) were treated i.p. ± OI (50 mg/kg) in 40% cyclodextrin in PBS or vehicle control for 2 h prior to stimulation with LPS (5 mg/kg) and monitored for temperature at 1, 2, 3, 4, 6, 12, 18 and 24 hours post LPS. Temperature was monitored using subcutaneously implanted temperature transponder chips (Bio Medic Data Systems; IPTT 300) which were injected between the shoulder blades 48 hours prior to experiment. At defined time body temperature was measured by scanning the transponder with a corresponding BMDS Smart Probe. Animals were additionally monitored for clinical signs of endotoxic shock, based on temperature change, body condition, physical condition and unprovoked behavior, with a combined score of 9 indicating the humane end point for the experiment.

siRNA transfection of BMDMs

Cells were plated at $1x10^6$ cells/ml in 12 well plates overnight. On the day of transfection the media was replaced with 500 µl DMEM without P/S or FBS. Two eppendorfs/siRNA were prepared. Optimem (250 µl/well) was added to each tube. RNAimax (add 5 µl/well) was added to one set of tubes and siRNA (50 nM/well) was added to the second set of tubes. The tubes containing the siRNA was added to the tube with RNAimax, mixed well by pipetting and incubated for 15 min. The mix (500 µl) was added to each well. 24 h post transfection cells were treated as required.

Analysis of Keap1 modification by OI

Human embryonic kidney cells (HEK293Ts) were transfected with a pCMV6-Keap1 vector (Myc-DDK-tagged mouse Keap1) (OriGene). 24 h post-transfection, cells were treated with OI (500 µM) or vehicle control (PBS) for 4 h. Tagged-Keap1 was immunoprecipitated using an anti-FLAG antibody (Sigma) and protein A/G beads (Santa Cruz). After immunoprecipitation, bound Keap1 was eluted off the beads using FLAG peptide (500 µl; 200 µg/ml) (Sigma) diluted in 1X TBS pH 7.4. The samples were then concentrated and the FLAG peptide removed using 10K centrifugation filter columns (Merck). The concentrated samples were then divided in half for downstream processing. One half of each sample was diluted 1 in 2 with 5X SDS sample buffer and separated using SDS-PAGE (Bio-Rad). Overexpressed Keap1 was detected using Coomassie blue staining and the corresponding bands were excised from the gel and subjected to in-gel digest as described. Briefly, the gel slices were cut into smaller pieces (1-2 mm^3) prior to reduction with DTT (10 mM) and alkylation with IAA (50 mM).

Half of the gel slices from each sample were then subjected to a trypsin (2 µg) digest, the other half were digested with elastase (1 µg) overnight at 37°C. Similarly, the remaining sample concentrates (in solution) were reduced with DTT and alkylated with IAA, prior to precipitation of the protein via the methanol-chloroform extraction method. The protein pellet was re-suspended in urea (6 M), which was then diluted to <1 M urea with ultrapure H_2O. The samples were then digested with trypsin (2 µg) overnight at 37°C. Digested protein samples were analysed in an Orbitrap Fusion Lumos coupled to a UPLC ultimate 3000 RSLCnano System (both Thermo Fisher). For further details see Supplementary Methods.

Assessment of cysteine alkylation by itaconate using Iodo-TMT

Following treatment cells were lysed in HEPES pH 7.5, EDTA, glycerol and NP40. 2 mM TCEP and 50 mM NEM were added in a buffer containing 50 mM HEPES, 2% SDS, 125 mM NaCl, pH 7.2 and samples were incubated for 60 min at 37 °C in the dark to reduce and alkylate all unmodified protein cysteine residues. 20% (v/v) TCA was added to stabilize thiols and incubated overnight at 4°C and then pelleted for 10 min at 4000 g at 4 °C. The pellet was washed with 3 times with cold methanol (2 ml) and then resuspended in 2 ml 8 M urea containing 50 mM HEPES (pH 8.5). Protein concentrations were measured by BCA assay (Thermo Scientific) prior to protease digestion. Protein lysates were diluted to 4 M urea and digested with LysC (Wako, Japan) in a 1/100 enzyme/protein ratio and trypsin (Promega) at a final 1/200 enzyme/protein ratio for 4 hours at 37 °C. Protein extracts were diluted further to a 2.0 M urea and LysC (Wako, Japan) at 1/100 enzyme/protein ratio and trypsin (Promega) at a final 1/200 enzyme/protein ratio were added again and incubated overnight at 37 °C. Protein extracts were diluted further to a 1.0 M urea concentration, and trypsin (Promega) was added to a final 1/200 enzyme/protein ratio for 6 hours at 37 °C. Digests were acidified with 250 µL of 25% acetic acid to a pH ~2, and subjected to C18 solid-phase extraction (50 mg Sep-Pak, Waters). 6-7 M excess TMT label was added to each digest for 30 min at room temperature (repeated twice). The reaction was quenched using 4 uL of 5% hydroxylamine.

Samples were subjected to an additional C18 solid-phase extraction (50 mg SepPak, Waters). For LC-MS/MS parameters, Data processing and MS2 spectra assignment, TMT reporter ion intensities and quantitative data analysis see Supplementary Methods.

Reagents

For a complete list of reagents see Supplementary Methods.

Mouse strains

Wild type C57Bl/6 mice were from Harlan U.K. and Harlan Netherlands. Animals were maintained under specific pathogen-free conditions in line with Irish and European Union regulations. Experiments were approved by local ethical review and were carried out under the authority of Ireland's project license. All animal studies performed in GSK were ethically reviewed and carried out in accordance with Animals (Scientific Procedures) Act 1986 and the GSK Policy on the Care, Welfare and Treatment of

Animals." Nrf2-deficient mice and their wild type counterparts, both on the C57Bl/6 genetic background (used for isolation of BMDM cells) were bred and maintained in the Medical School Resource Unit of the University of Dundee.

Statistical analysis

Data were expressed as mean ± s.e.m. and *P* values were calculated using twotailed Student's t-test for pairwise comparison of variables, one-way ANOVA for multiple comparison of variables, and two-way ANOVA involving two independent variables. A Sidak's multiple comparisons test was used. A confidence interval of 95% was used for all statistical tests. Sample sizes were determined on the basis of previous experiments using similar methodologies. For all experiments, all stated replicates are biological replicates. For *in vivo* studies, mice were randomly assigned to treatment groups. For MS analyses, samples were processed in random order and experimenters were blinded to experimental conditions.

Data Availability

Full scans for all western blots have been provided in the Supplementary Figures. Source Data for all mouse experiments have been provided. All other data are available from the corresponding author on reasonable request.

References

26 Chappell, J. B., Hansford, R. V. A. *Subcellular components: preparation and fractionation*. 2nd edn, (Butterworth, 1972).

27 Bridges, H. R., Mohammed, K., Harbour, M. E. & Hirst, J. Subunit NDUFV3 is present in two distinct isoforms in mammalian complex I. *Biochimica et biophysica acta* **1858**, 197-207, doi:10.1016/j.bbabio.2016.12.001 (2017).

28 Akerboom, T. P. & Sies, H. Assay of glutathione, glutathione disulfide, and glutathione mixed disulfides in biological samples. *Methods in enzymology* **77**, 373-382 (1981).

29 Booty, L. M. *et al.* The mitochondrial dicarboxylate and 2-oxoglutarate carriers do not transport glutathione. *FEBS letters* **589**, 621-628, doi:10.1016/j.febslet.2015.01.027 (2015).

Extended Data Figure 1. The effect of itaconate on CII activity. a Complex II+III activity in bovine heart mitochondrial membranes incubated with succinate ± malonate or itaconate (*n*=3 independent experiments). **b** Effect of malonate or itaconate on oxygen consumption rate of rat liver mitochondria in the presence of succinate (1 mM) and FCCP (1 µM; *n*=3 independent experiments). **c, d** Complex II+III activity in bovine heart mitochondrial membranes incubated with itaconate (1 mM unless indicated), with subsequent removal and addition of succinate (1 mM; *n*=3 independent experiments). Data are mean ± s.e.m, *n*=3 independent experiments. *P* values calculated using one or two-way ANOVA.

Extended Data Figure 2. DMI activates Nrf2 and limits cytokine production. a, c LPS (100 ng/ml)-induced Nrf2 (**a**, 24 h) and Hmox1 (**c**, 6 h) protein expression ± DMI. **b** Nrf2-dependent mRNA expression ± LPS (6 h) ± DMI (*n*=3). **d** GSH and GSSG levels ± LPS ± DMI (*n*=5). **e, f** LPS (24 h)-induced IL-1β mRNA (**e**), IL-1β and HIF-1α protein (**f**) expression ± DMI (*n*=3). Data are mean ± s.e.m. *P* values calculated using one-way ANOVA. Blots are representative of 3 independent experiments. For gel source data, see Supplementary Figure 1.

Extended Data Figure 3. OI is the best tool to assess itaconate-dependent Nrf2 activity. a Reactivity of DMI, itaconate and OI with thiols. **b, c** Itaconate ester reactivity with GSH ± GST as detailed in Methods (*n*=3). **d** Itaconate levels in C2C12 cells ± itaconate esters (*n*=3). **e, i** Itaconate or GSH levels ± LPS (6 h) ± OI (*n*=5). **f** NQO1 activity in Hepa1c1c7 cells treated with DMI or OI (48 h) ± GSH (*n*=8). **g, h** Metabolic intermediates in glutathione (GSH) synthesis (**h**, average of 5 biological replicates). **i** GSH levels ± LPS (6 h) ± OI (*n*=5). j GSH/GSSG ± OI (2 h) ± H_2O_2 (100 µM, 24 h; *n*=3). **k** Hmox protein levels ± OI ± H_2O_2 (24 h). **l** Nrf2, Hmox and IL-1β protein levels in BMDMs pre-treated with OI, 4-octyl 2-methylsuccinate (OMS) or octyl succinate (OS), all 125 µM for 3 h ± LPS (6 h). **m** LPS-induced Nrf2 (24 h) and Hmox1 (6 h) protein expression ± dimethyl malonate (DMM). Data are mean ± s.e.m. *P* values calculated using one- or two-way ANOVA. Blots are representative of 3 independent experiments. For gel source data, see Supplementary Figure 1.

Extended Data Figure 4. Itaconate is transported by the mitochondrial oxoglutarate, dicarboxylate and citrate carriers. a Itaconate uptake into vesicles of *Lactococcus lactis* membranes expressing indicated carriers loaded with itaconate (1 mM), and transport initiated by the addition of [^{3}H]-itaconate (1 µM). **b** Initial transport rates of each carrier with either canonical substrate (homo-exchange) or canonical substrate/itaconate (hetero-exchange). Results are presented as *n*=4 independent experiments ± S.D. *P* values calculated using 2-tailed student t-test.

Extended Data Figure 5. Keap1 is alkylated by OI on major redox sensing cysteines. a Modification of cysteine by fumarate or itaconate. MS/MS spectrum of Keap1 Cys257 (**b**), Cys257 (**c**) and Cys288 (**d**) peptides indicating alkylation of these sites with OI treatment (left) but not in the corresponding carbamidomethylated (CAM) peptides (right). **e, f** Ldha Cys84 alkylation ± LPS (**e**, 24 h) or OI (**f**, 250 µM, 4 h) (*n*=4). Detected N- and C-terminal fragment ions of both peptides are assigned in the spectrum and depicted as follows: b: N-terminal fragment ion; y: C-terminal fragment ion; *: fragment ion minus NH_3; 0 or *: fragment ion minus H_2O; and 2+: doubly charged fragment ion. Representative of 1 independent experiment.

Extended Data Fig 6. Identification of an itaconate-cysteine adduct. $^{13}C_6$-glucose (**a-c**) or $^{13}C_5$-glutamine (**d-e**) labelling experiment tracking itaconate-cysteine adduct formation in BMDMs treated with LPS (*n*=5; 24 h). **b, e** represent % isotopologue of the total pool. **c, f** represent changes in the total pool ± LPS treatment. Data are mean ± s.e.m, for 5 replicates. *P* values calculated using two-way ANOVA.

Extended Data Figure 7. OI decreases LPS-induced cytokine production, ECAR, ROS and NO. a % cytotoxicity in BMDMs ± LPS ± OI (*n*=3). **b** LPS-induced ECAR ± OI, analysed on the Seahorse XF-24 in BMDMs (representative trace of *n*=3). **c, d** LPS-induced IL-10 mRNA (**c**, 4 h) and protein (**d**, 24 h) and TNF-α protein (**f**; *n*=7) ± OI (*n*=3). **e** pp65 protein levels ± LPS ± OI. **h** Representative gating strategy for FACS analysis of ROS production in cells as treated in **d** (representative image of *n*=3). **i** LPS-induced Nos2 expression (*n*=6) ± OI. **j** LPS-induced TNF-α (*n*=4) and IL-1β (*n*=3) protein levels ± OI in PBMCs. **k** Nrf2 and hmox1 protein levels (m=mouse) or Nrf2-dependent gene expression (*n*=5) in peritoneal macrophages from mice i.p. injected ± OI (50 mg/kg, 6 h). **l** Serum IL-10 from mice i.p. injected ± OI (50 mg/kg, 2 h) ± LPS (2.5 mg/kg, 2 h, *n*=3 vehicle, OI; *n*=15 LPS, OI+LPS). Data are mean ± s.e.m. *P* values calculated using one-way ANOVA. Blots are representative of 3 independent experiments. For gel source data, see Supplementary Figure 1.

Extended Data Figure 8. The effects of OI on cytokine production are Nrf-2dependent. a-e: Nrf2, Hmox1, IL-1β protein (**a, c, d**) and IL-1β mRNA (**b, e**) expression in BMDMs transfected with two different Nrf2 (50 nM) siRNAs compared with non-silencing control ± LPS (6 h; **a, b, d**) or (24 h; **c, d, e**) ± OI (*n*=6). **f** IL-1β mRNA expression in wild-type and Nrf2 KO BMDMs treated with LPS (24 h; WT (*n*=2) and Nrf2 KO (*n*=4)) ± OI. IL-1β (**g**), Nos2 (**j**) mRNA and IL-1β (**h**), IL-10 (**i**),
TNF-α and NO (**k**) protein ± LPS (24 h) ± diethyl maleate (DEM; 100 µM) or 15Deoxy-Δ12,14-prostaglandin J2 (J2; 5 µM) pretreatment for 3 h (*n*=3). Data are mean ± s.e.m. *P* values calculated using one-way ANOVA. Blots are representative of 3 independent experiments. For gel source data, see Supplementary Figure 1.

Extended Data Figure 9. An Nrf2-dependent feedback loop exists between itaconate and IFN-β. a Metabolite levels ± IFN-β (1000 U/ml; 27 h; *n*=5). **b, c** Isg20 and Irf5 mRNA expression in BMDMs treated with LPS (**b**) or poly I:C (**c**, 40 µg/ml; 24 h) ± OI (*n*=6). **d** IL-10 mRNA (*n*=3) and protein (*n*=5) expression ± LPS for 4 h (left panel) or 24 h (right panel) ± IFN-β treatment (1000 U/ml) for 3 h. **e** Isg20 expression in BMDMs transfected with two different Nrf2 (50 nM) siRNAs compared with non-silencing control ± LPS (6 h) ± OI (*n*=6). **f** ISG20 mRNA expression in WT (*n*=2) and Nrf2 KO (*n*=4) BMDMs ± LPS (6 h) ± OI. **g** ISG20 mRNA expression ± LPS (24 h) ± diethyl maleate (DEM; 100 µM) or 15-Deoxy-Δ12,14-prostaglandin J2 (J2; 5 µM) pretreatment for 3 h (*n*=3). Data are mean ± s.e.m, *P* values calculated using one-way ANOVA.

Extended Data Table 1. Mass spectrometry analysis of itaconate-induced cysteine alkylation. **a** Cysteine/Lysine Residue(s) in Keap1 modified by OI as determined by tandem mass spectrometry. **b** Cysteine residues modified by itaconate in BMDMs treated with LPS identified using tandem mass spectrometry. **c** Cysteine residues modified by itaconate in BMDMs treated with OI identified using tandem mass spectrometry

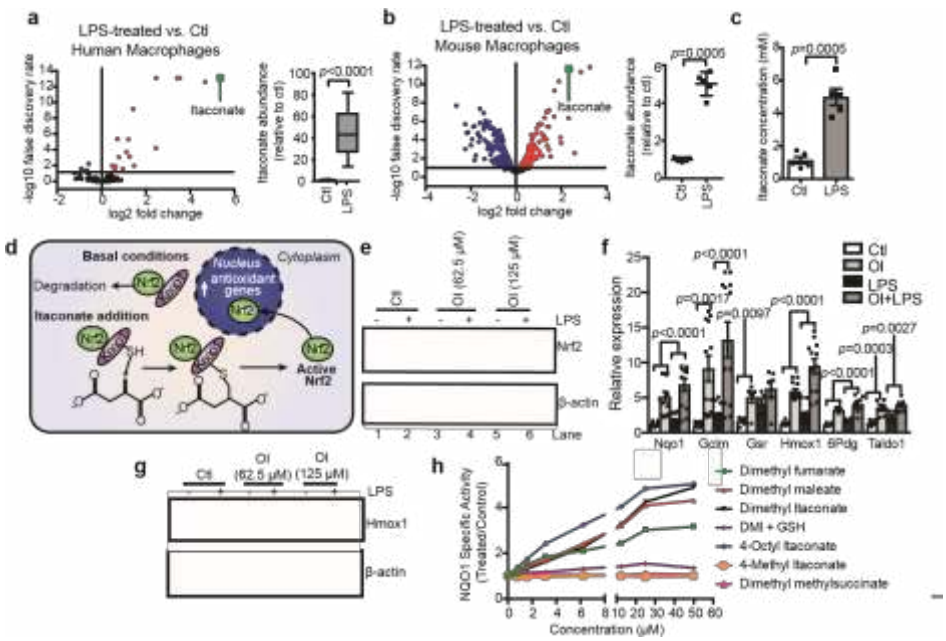
a
LPS-treated vs. Ctl
Human Macrophages
-log10 false discovery rate
log2 fold change
Itaconate
Itaconate abundance (relative to ctl)
p<0.0001
Ctl
LPS
b
LPS-treated vs. Ctl
Mouse Macrophages
-log10 false discovery rate
log2 fold change
Itaconate
Itaconate abundance (relative to ctl)
p=0.0006
c
Itaconate concentration (mM)
p=0.0005
d
Basal conditions
Cytoplasm
Nucleus
antioxidant genes
Degradation
Itaconate addition
SH
Active Nrf2
e
Ctl
OI (62.5 μM)
OI (125 μM)
LPS
Nrf2
β-actin
Lane
f
Ctl
OI
LPS
OI+LPS
Relative expression
p<0.0001
p=0.0017
p=0.0097
p<0.0001
p=0.0027
p=0.0003
p<0.0001
Nqo1
Gclm
Gsr
Hmox1
6Pdg
Taldo1
g
Ctl
OI (62.5 μM)
OI (125 μM)
LPS
Hmox1
β-actin
h
NQO1 Specific Activity (Treated/Control)
Concentration (μM)
Dimethyl fumarate
Dimethyl maleate
Dimethyl itaconate
DMI + GSH
4-Octyl itaconate
4-Methyl itaconate
Dimethyl methylsuccinate

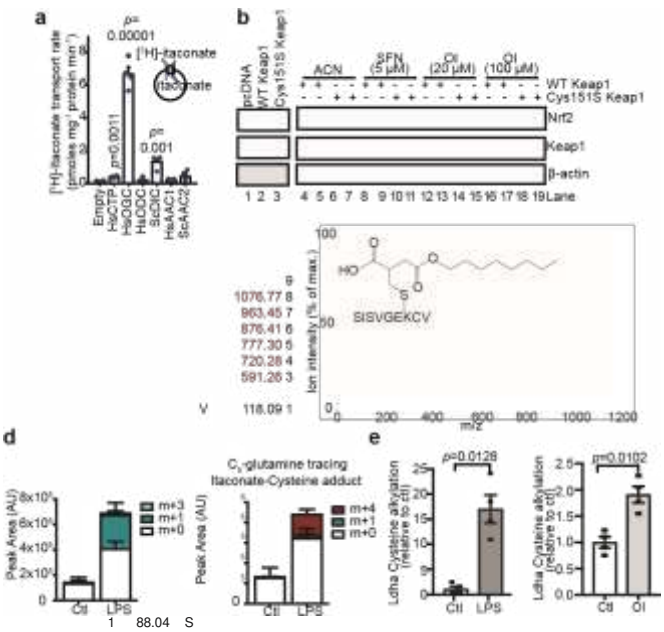

1	88.04	S	
2	201.07	I	3
288.20		S	4
378.29		V	5
444.22		G	6
573.25		E	7
701.28	K		
8	1046.44	C(+242.15)	463.17 2
9			

$^{13}C_6$-glucose tracing to Itaconate-Cysteine adduct

13

1x10
8x10
6x10
4x10
2x10

c

b-ions	Sequence	y-ions

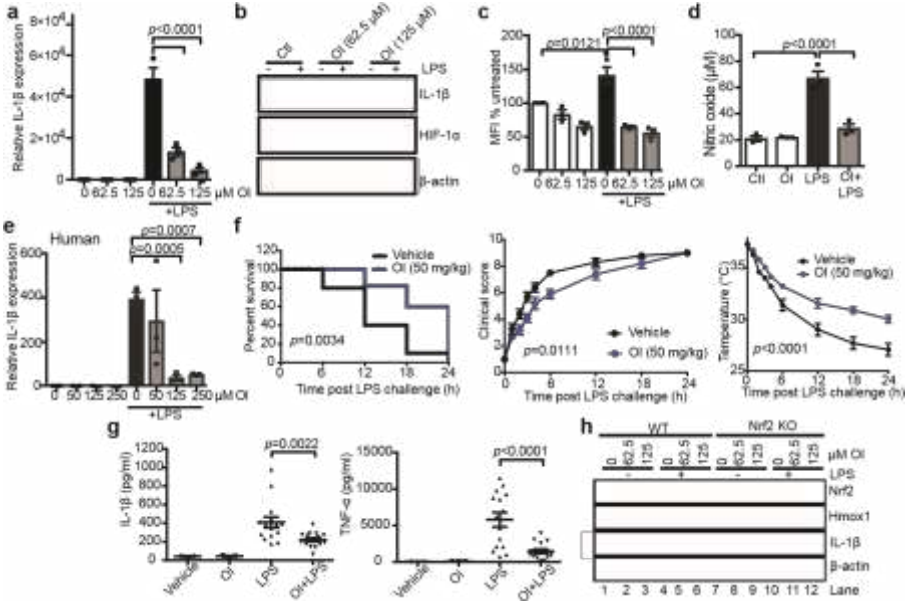
a
Relative IL-1β expression
p<0.0001
0 62.5 125 0 62.5 125 μM OI
+LPS
b
Ctl
OI (62.5 μM)
OI (125 μM)
LPS
IL-1β
HIF-1α
β-actin
c
MFI % untreated
p=0.0121
p<0.0001
0 62.5 125 0 62.5 125 μM OI
+LPS
d
Nitric oxide (μM)
p<0.0001
Ctl
OI
LPS
OI+ LPS
e
Human
p=0.0007
p=0.0006
Relative IL-1β expression
0 50 125 250 0 50 125 250 μM OI
+LPS
f
Vehicle
OI (50 mg/kg)
Percent survival
p=0.0034
Time post LPS challenge (h)
Clinical score
p=0.0111
Vehicle
OI (50 mg/kg)
Time post LPS challenge (h)
Temperature (°C)
Vehicle
OI (50 mg/kg)
p<0.0001
Time post LPS challenge (h)
g
IL-1β (pg/ml)
p=0.0022
Vehicle
OI
LPS
OI+LPS
TNF-α (pg/ml)
p<0.0001
Vehicle
OI
LPS
OI+LPS
h
WT
Nrf2 KO
0 62.5 125 0 62.5 125 0 62.5 125 0 62.5 125 μM OI
LPS
Nrf2
Hmox1
IL-1β
β-actin
1 2 3 4 5 6 7 8 9 10 11 12 Lane

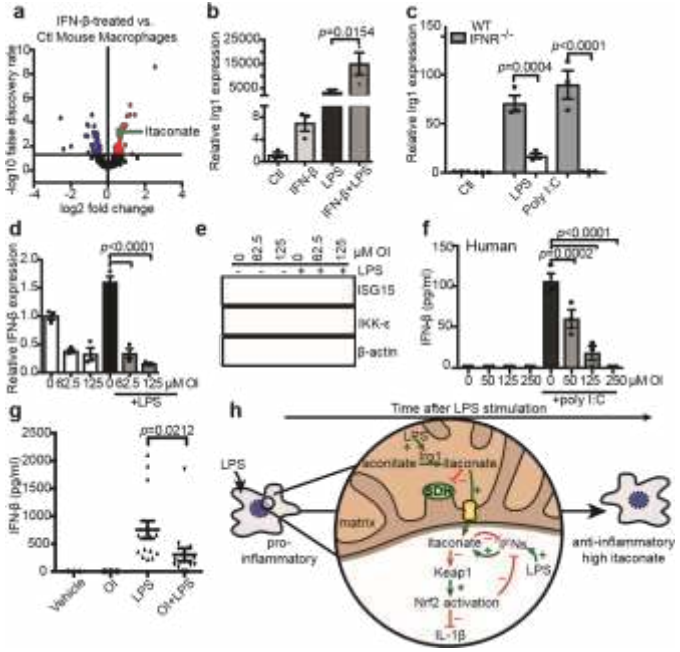
a
IFN-β-treated vs.
Ctl Mouse Macrophages
-log10 false discovery rate
log2 fold change
Itaconate
b
Relative Irg1 expression
p=0.0154
Ctl
IFN-β
LPS
IFN-β+LPS
c
WT
IFNR-/-
Relative Irg1 expression
p=0.0004
p<0.0001
Ctl
LPS
Poly I:C
d
Relative IFN-β expression
p<0.0001
0 62.5 125 0 62.5 125 μM OI
+LPS
e
10 62.5 125 0 62.5 125 μM OI
LPS
ISG15
IKK-ε
β-actin
f
Human
p<0.0001
p=0.0002
IFN-β (pg/ml)
0 50 125 250 0 50 125 250 μM OI
+poly I:C
g
IFN-β (pg/ml)
p=0.0212
Vehicle
Ctl
LPS
Ctl+LPS
h
Time after LPS stimulation
LPS
pro-inflammatory
LPS
+
Irg1
aconitate
itaconate
SDH
matrix
itaconate
IFNs
Keap1
LPS
Nrf2 activation
IL-1β
anti-inflammatory
high itaconate

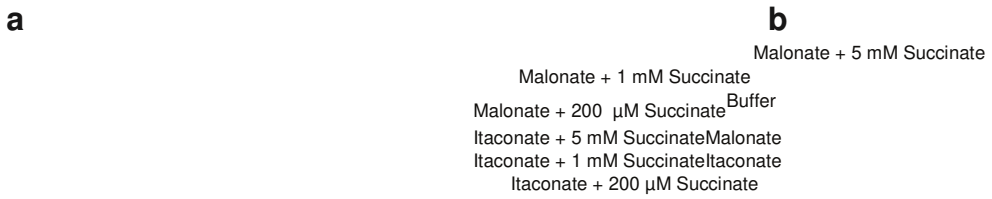

c **d**

Extended Data Figure 1. The effect of itaconate on CII activity. a Complex II+III activity in bovine heart mitochondrial membranes incubated with succinate ± malonate or itaconate (*n*=3). **b** Effect of malonate or itaconate on oxygen consumption rate of rat liver mitochondria in the presence of succinate (1 mM) and FCCP (1 µM; *n*=3). **c, d** Complex II+III

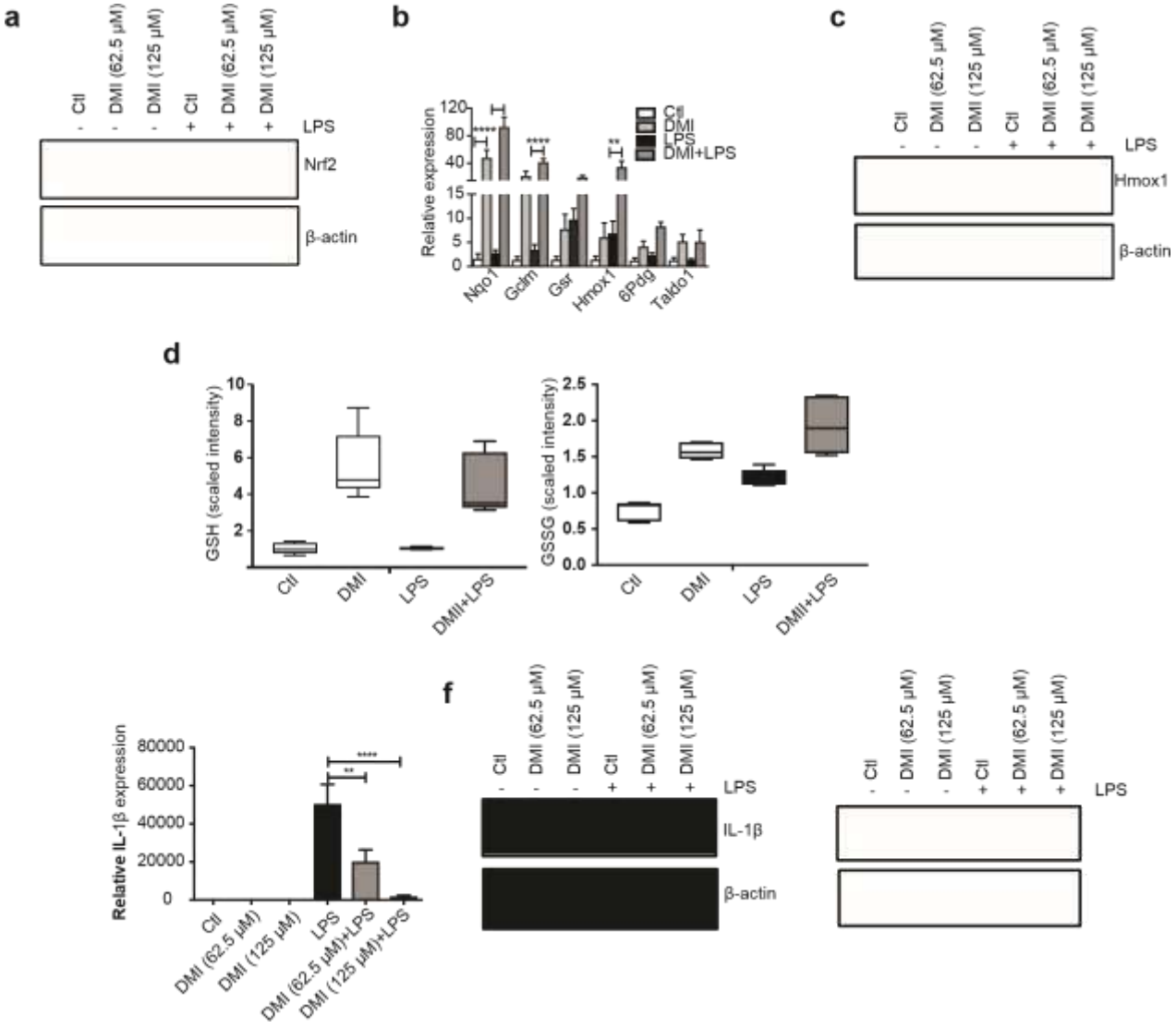

activity in bovine heart mitochondrial membranes incubated with itaconate (1 mM unless indicated), with subsequent removal and addition of succinate (1 mM; *n*=3)). Data are mean ± s.e.m, *n*=3. *P<0.05, **P<0.01, ***P<0.001, ****P<0.0001 one or two-way ANOVA.

****

e

HIF-1α

β-actin

Extended Data Figure 2. DMI activates Nrf2 and limits cytokine production. a, c LPS (100 ng/ml)-induced Nrf2 (**a**, 24 h) and Hmox1 (**c**, 6 h) protein expression ± DMI pretreatment for 3 h. **b** Nrf2-dependent mRNA expression in LPS-stimulated BMDMs (6 h) ± DMI (125 μM) pretreatment for 3 h (*n*=3). **d** GSH and GSSG levels in LPS (100 ng/ml)-treated BMDMs ± DMI pretreatment for 3 h (*n*=5). **e, f** LPS (100 ng/ml, 24 h)-induced IL-1β mRNA (**e**), IL-1β and HIF-1α protein (**f**) expression ± DMI pretreatment for 3 h in BMDMs (*n*=3). Data are mean ± s.e.m, of at least 3 replicates. **p<0.01, ****p<0.0001 one-way ANOVA. Blots are representative of 3 experiments.

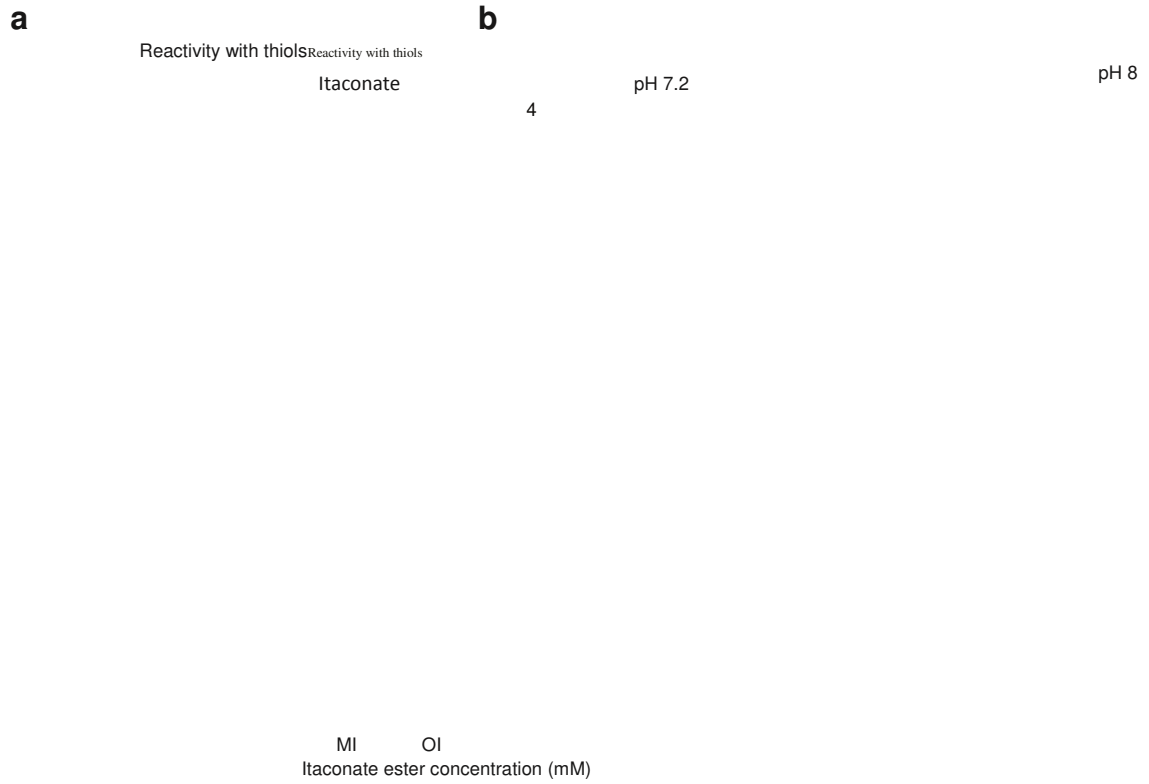

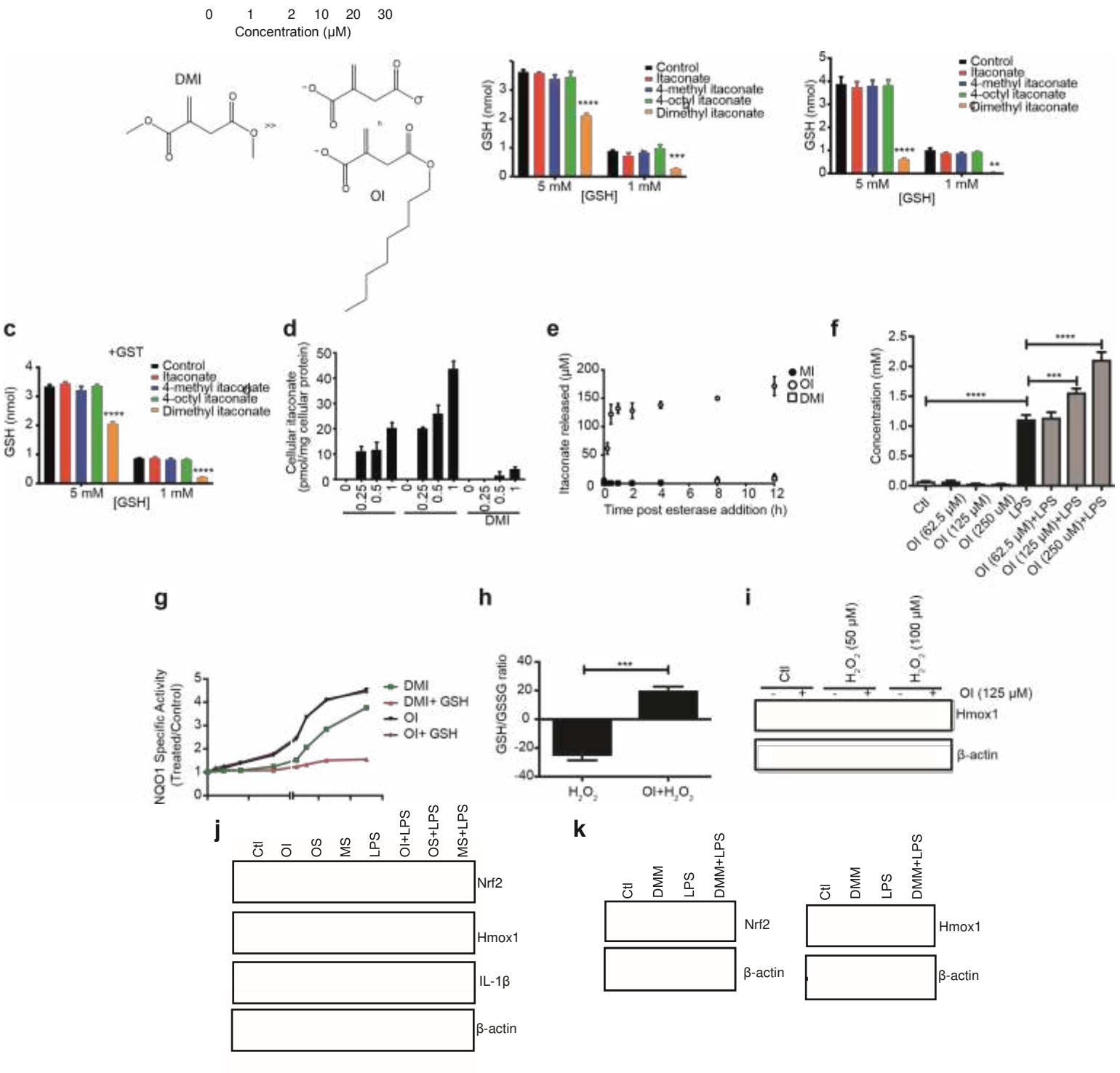

Extended Data Figure 3. OI is the best tool to assess itaconate-dependent Nrf2 activity. a Schematic of reactivity of DMI versus itaconate or OI with thiols. **b, c** Itaconate ester reactivity with GSH ± GST as detailed in Methods (*n*=3). **d** LC-MS/MS analysis of itaconate levels in C2C12 cells treated with itaconate esters (*n*=3). **e** LC-MS/MS analysis of itaconate release following incubation of itaconate esters with porcine liver esterase (*n*=3). **f, h** Absolute quantification of itaconate levels (**f**) or relative GSH levels (fold over ctl; **h**) in BMDMs treated with LPS (100 ng/ml) for 6 h ± OI pretreatment for 3 h (*n*=5). **g** NQO1 activity in Hepa1c1c7 cells treated with DMI or OI for 48 h ± GSH pre-treatment. NQO1 activity was determined as described in Methods (*n*=8). **h** GSH/GSSG ratio in BMDMs pre-treated with OI (125 μM) for 2 h and then stimulated with H_2O_2 (100 μM) for 24 h (*n*=3) as determined using MyBio GSH/GSSG-Glo Assay. **i** Hmox protein levels in BMDMs pre-treated with OI (125 μM) for 3 h and then stimulated with H_2O_2 for 24 h. **j** Nrf2, Hmox and IL-1β protein levels in BMDMs pre-treated with 4-octyl itaconate (OI), 4-octyl 2-methylsuccinate (MS) or octyl succinate (OS;

125 μM), for 3 h and then stimulated with LPS (100 ng/ml) for 6 h. **k** LPS (100 ng/ml)-induced Nrf2 (24 h) and Hmox1 (6 h) protein expression ± DMM pretreatment for 3 h. Data are mean ± s.e.m of at least 3 replicates. *P<0.05, **P<0.01, ***P<0.001, ****P<0.0001 one- or two-way ANOVA.

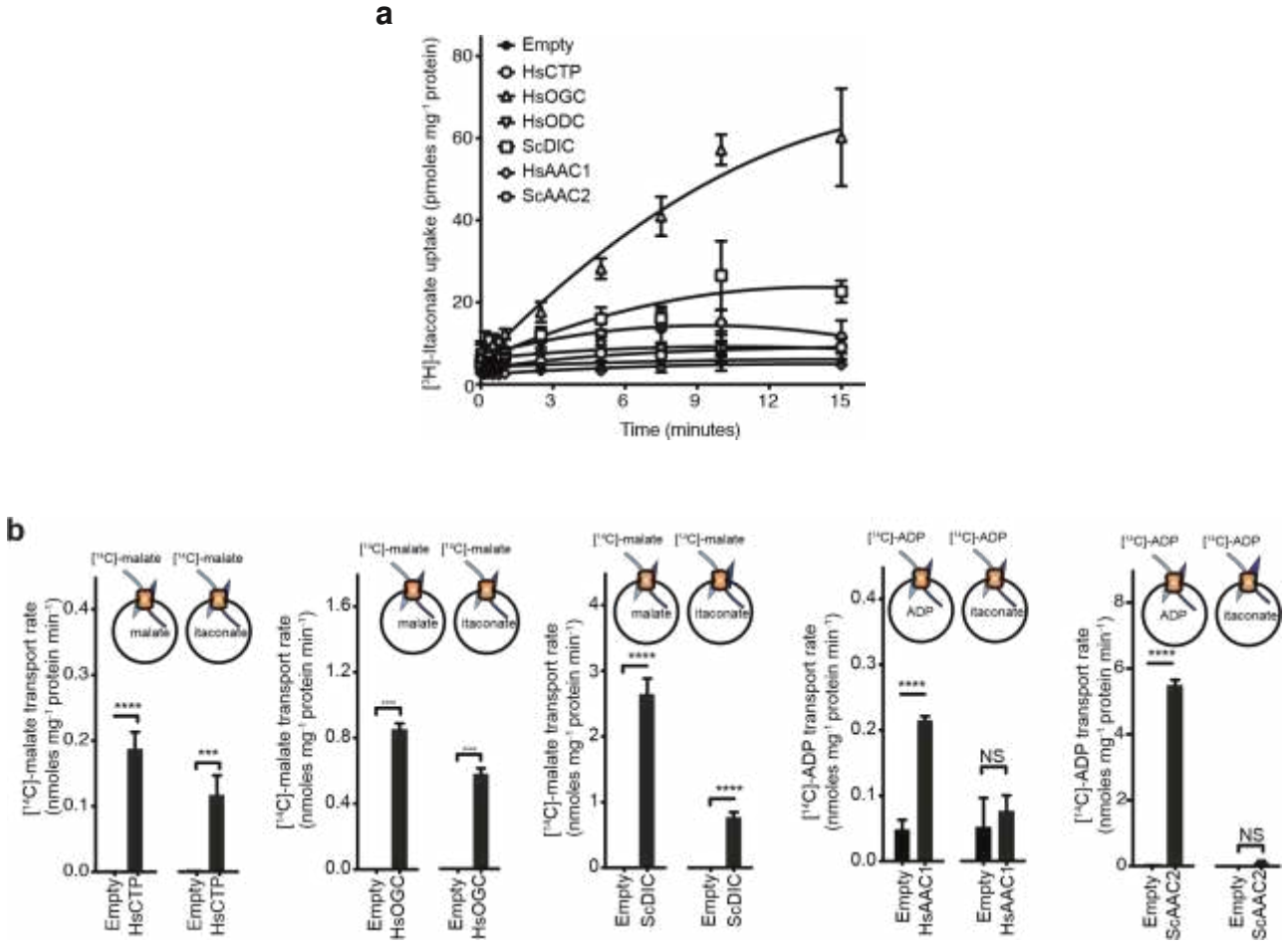

Extended Data Figure 4. Itaconate is transported by the mitochondrial oxoglutarate, dicarboxylate and citrate carriers. a Itaconate uptake into vesicles of Lactococcus lactis membranes expressing indicated carriers loaded with itaconate (1 mM), and transport initiated by the addition of [3H]-itaconate (1 μM). **b** Initial transport rates of each carrier with either canonical substrate (homo-exchange) or canonical substrate/itaconate (hetero-exchange, as indicated in each panel. Empty vector control rates are also shown. For details see Methods. Results are presented as n=4 ± S.D. *P<0.05, **P<0.01, ***P<0.001, ****P<0.0001 student t-test.

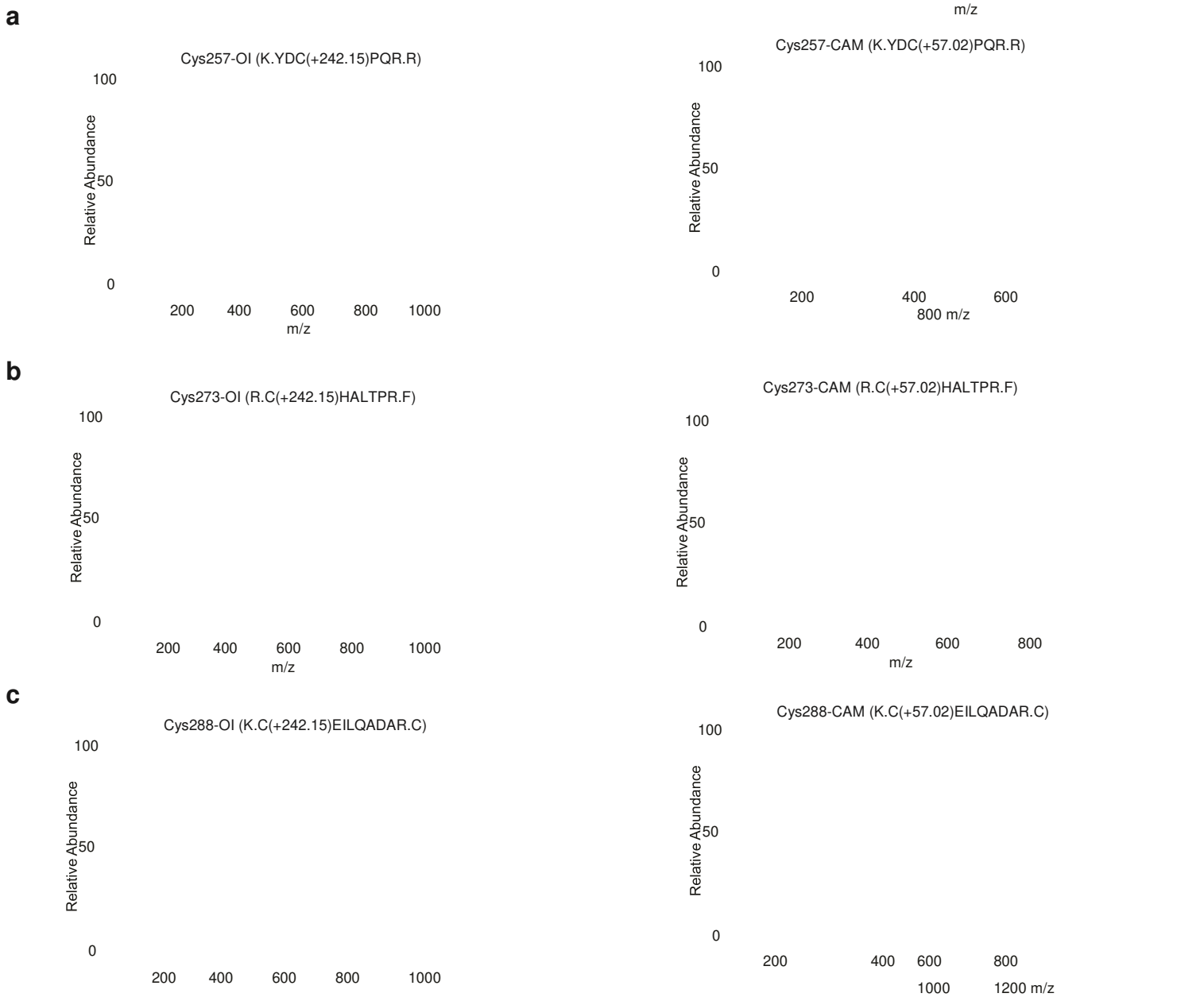

Extended Data Figure 5. Keap1 is alkylated by OI on major redox sensing cysteines. MS/MS spectrum of Keap1 Cys257 (**a**), Cys257 (**b**) and Cys288 (**c**) peptides indicating alkylation of these sites with OI treatment (left) but not in the corresponding carbamidomethylated (CAM) peptides (right). Detected N- and C-terminal fragment ions of both peptides are assigned in the spectrum and depicted as follows: b: N-terminal fragment ion; y: C-terminal fragment ion; *: fragment ion minus NH_3; ^{0}: fragment ion minus H_2O; and $^{2+}$: doubly charged fragment ion.

a

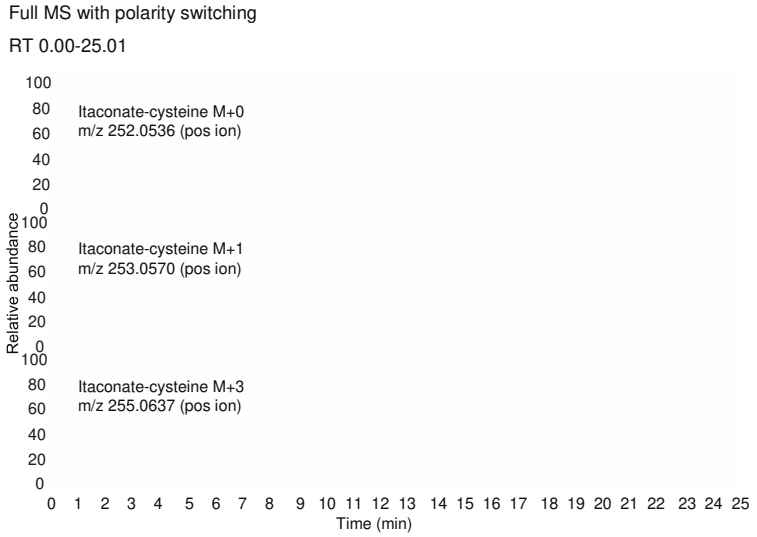

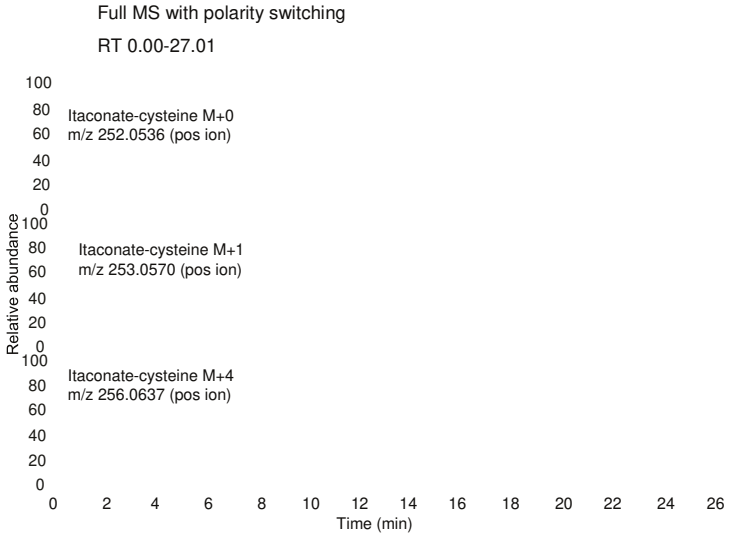

b

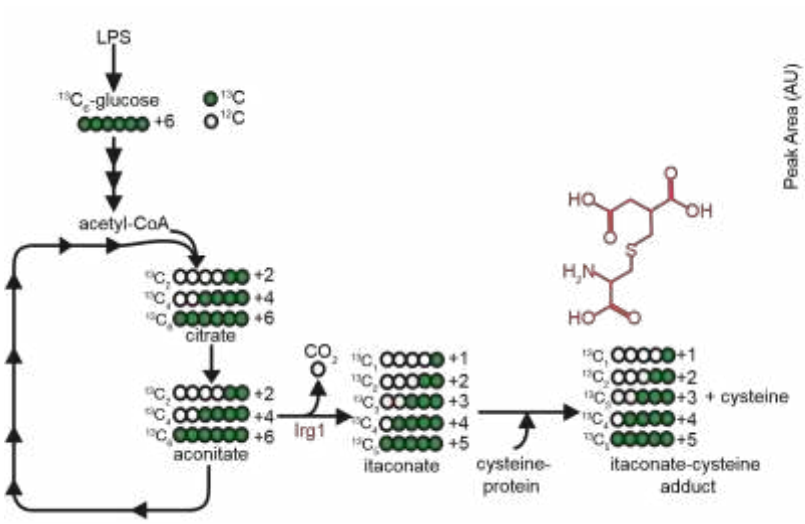

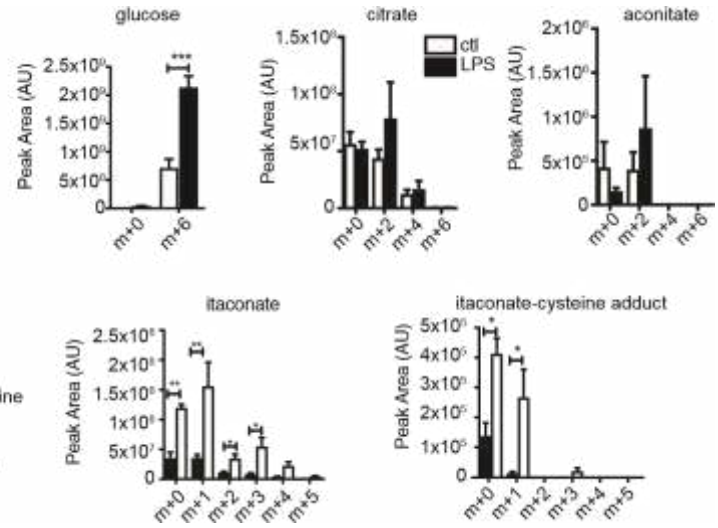

c

succinate

O

glutamine

α-KG

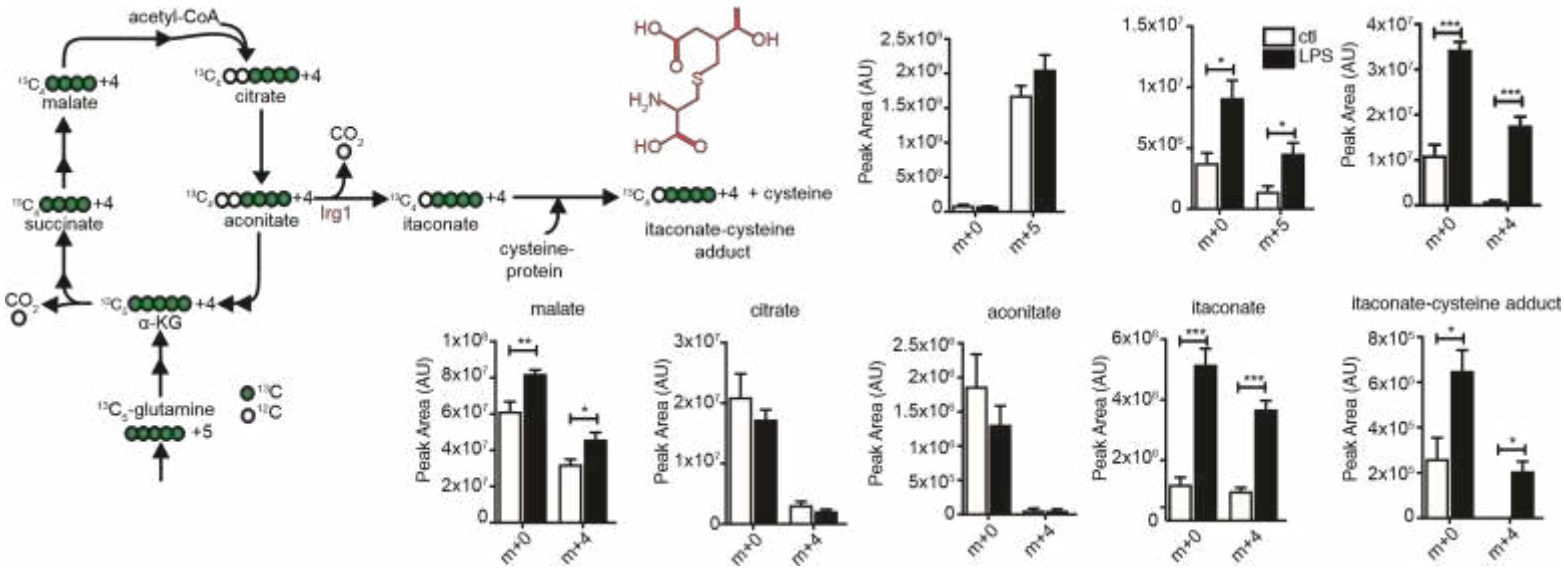

LPS

Extended Data Fig 6. Identification of an itaconate-cysteine adduct. a MS/MS spectrum of itconate-cysteine adduct in LPS treated macrophages treated with $^{13}C_6$-glucose (left) or $^{13}C_5$-glutamine (right). **b, c** Potential inputs to itaconate-cysteine adduct formation and ^{13}C-metabolite labelling strategy and $^{13}C_6$-glucose (**b**) or $^{13}C_5$-glutamine (**c**) profile of Krebs cycle intermediates and itaconate-cysteine adduct in BMDMs treated with LPS (100 ng/ml) for 24 h.

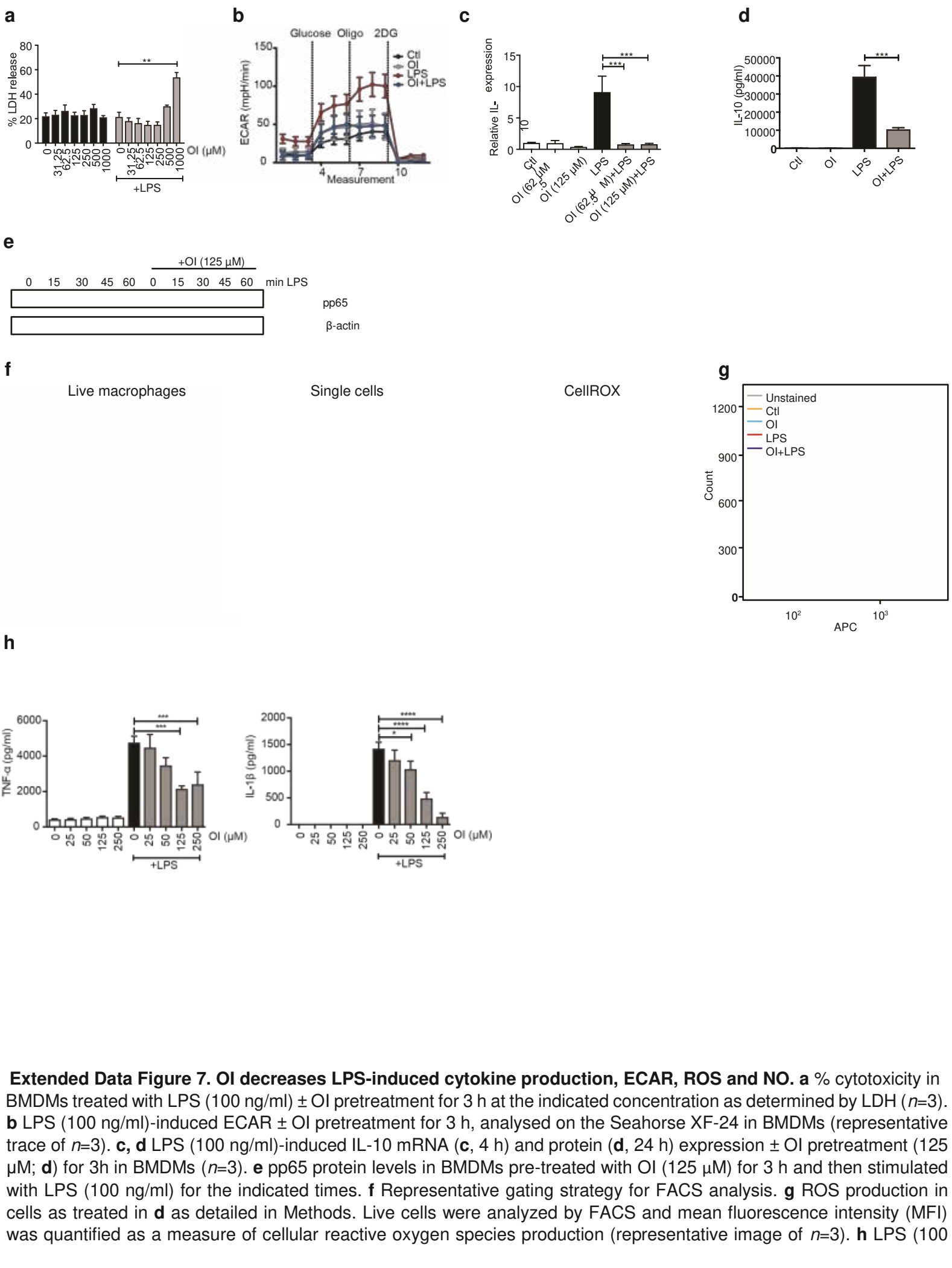

Extended Data Figure 7. OI decreases LPS-induced cytokine production, ECAR, ROS and NO. a % cytotoxicity in BMDMs treated with LPS (100 ng/ml) ± OI pretreatment for 3 h at the indicated concentration as determined by LDH (*n*=3). **b** LPS (100 ng/ml)-induced ECAR ± OI pretreatment for 3 h, analysed on the Seahorse XF-24 in BMDMs (representative trace of *n*=3). **c, d** LPS (100 ng/ml)-induced IL-10 mRNA (**c**, 4 h) and protein (**d**, 24 h) expression ± OI pretreatment (125 μM; **d**) for 3h in BMDMs (*n*=3). **e** pp65 protein levels in BMDMs pre-treated with OI (125 μM) for 3 h and then stimulated with LPS (100 ng/ml) for the indicated times. **f** Representative gating strategy for FACS analysis. **g** ROS production in cells as treated in **d** as detailed in Methods. Live cells were analyzed by FACS and mean fluorescence intensity (MFI) was quantified as a measure of cellular reactive oxygen species production (representative image of *n*=3). **h** LPS (100

ng/ml, 24 h)-induced TNF-α (*n*=4) and IL-1β (*n*=3) protein levels ± OI pretreatment for 3 h in PBMCs. Data are mean ± s.e.m, of at least 3 replicates. *p<0.05; **p<0.01, ***p<0.001, ****p<0.0001 one-way ANOVA. Blots are representative of 3 experiments.

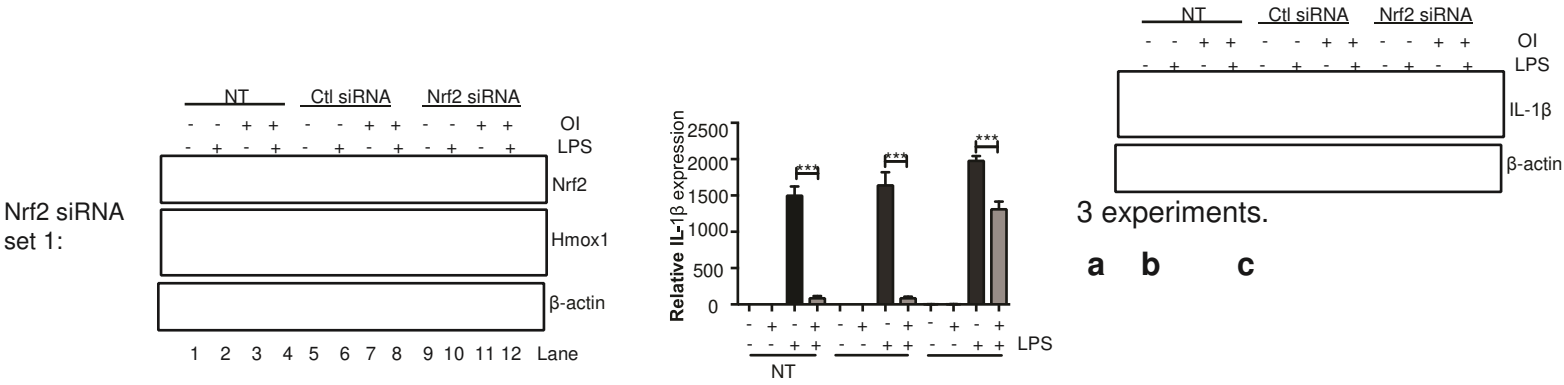

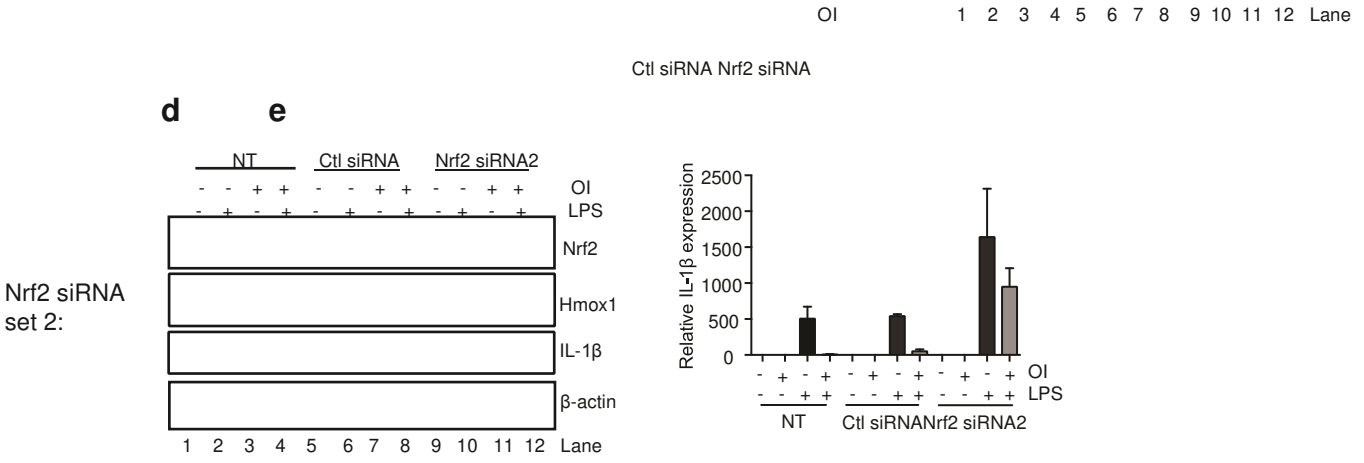

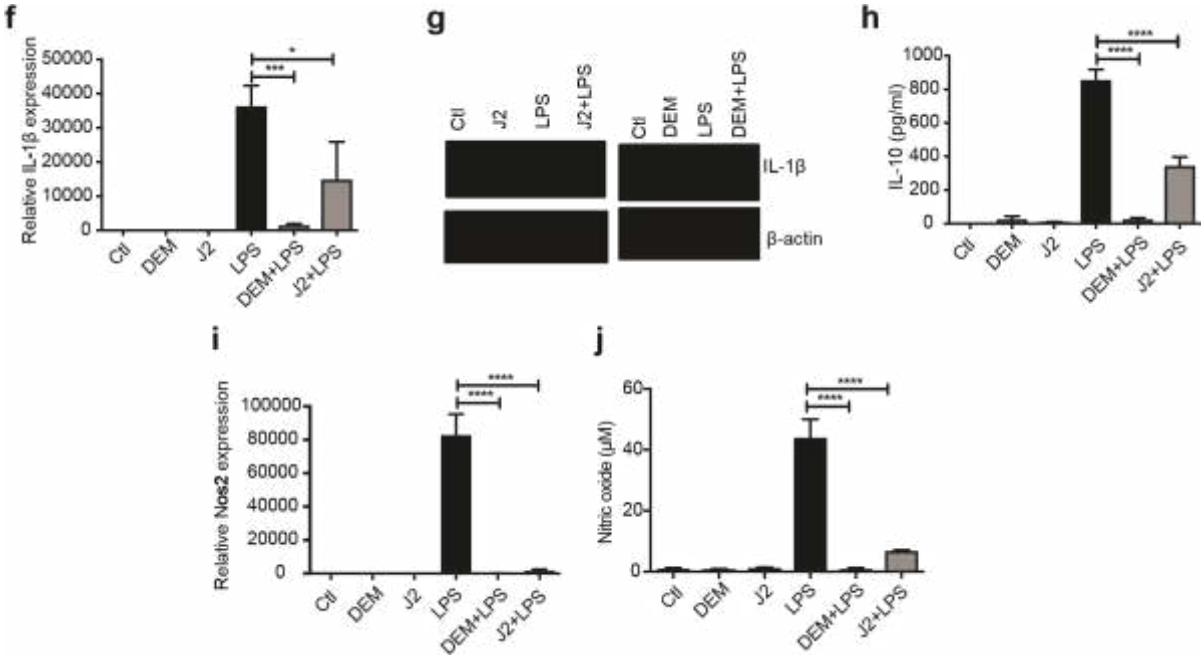

Extended Data Figure 8. The effects of OI on cytokine production are Nrf-2-dependent. a-e: Nrf2, Hmox1, IL-1β protein (**a, c, d**) and IL-1β mRNA (**b, e**) expression in BMDMs transfected with two different Nrf2 (50 nM) siRNAs compared with non-silencing control following treatment with LPS for 6 h (**a, b, d**) or 24 h (**c, d, e**) ± OI (125 μM) pretreatment for 3h (*n*=6). IL-1β (**f**), Nos2 (**i**) mRNA and IL-1β (**g**), IL-10 (**h**) and TNF-α protein expression in BMDMs treated with LPS for 24 h ± diethyl maleate (DEM; 100 μM) or 15-Deoxy-Δ12,14-prostaglandin J2 (J2; 5 μM) pretreatment for 3 h (*n*=3). **g** NO production in cells treated as in **f-j** using a Greiss reagent kit (*n*=3). Data are mean ± s.e.m, of at least 3 replicates. *p<0.05, ***p<0.001, ****p<0.0001 one-way ANOVA. Blots are representative of 3 experiments.

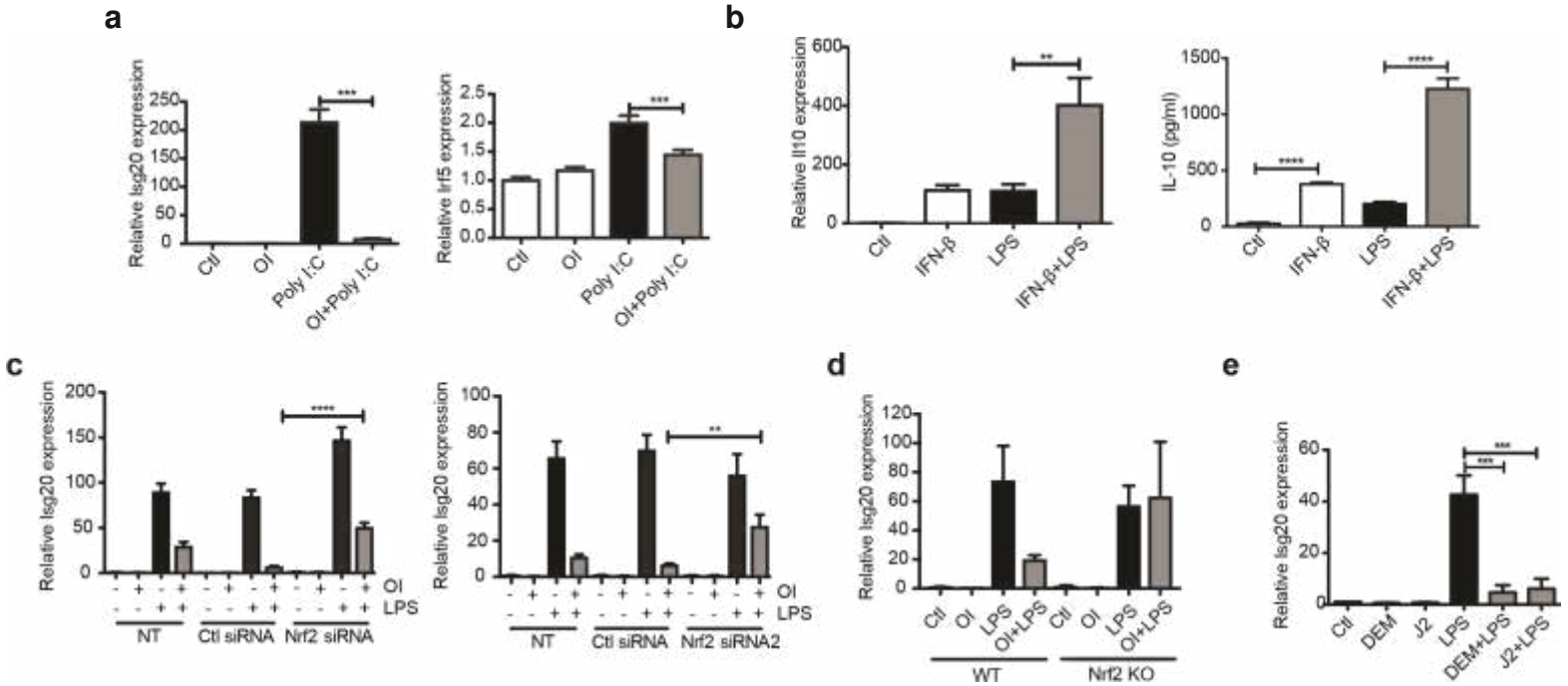

Extended Data Figure 9. An Nrf2-dependent feedback loop exists between itaconate and IFN-β. a Isg20 and Irf5 mRNA expression in BMDMs treated with poly I:C (40 μg/ml,) for 24 h ± OI pre-treatment (125 μM) for 3 h (*n*=6). **b** IL-10 mRNA (*n*=3) and protein (*n*=5) expression in BMDMs treated with LPS (100 ng/ml) for 4 (left panel) or 24 (right panel) ± IFN-β treatment (1000 U/ml) for 3 h. **c** Isg20 expression in BMDMs transfected with two different Nrf2 (50 nM) siRNAs compared with non-silencing control following treatment with LPS for 6 h ± OI (125 μM) pretreatment for 3 h (*n*=6). **d**

ISG20 mRNA expression in WT (*n*=2) and Nrf2 KO (*n*=4) BMDMs treated with LPS for 6 h ± OI (125 μM) pretreatment for 3 h. **e** ISG20 mRNA expression in BMDMs treated with LPS for 24 h ± diethyl maleate (DEM; 100 μM) or 15-Deoxy-Δ 12,14-prostaglandin J2 (J2; 5 μM) pretreatment for 3 h (*n*=3). Data are mean ± s.e.m, of at least 3 replicates. **p<0.01, ***p<0.001, ****p<0.0001 one-way ANOVA.

Table 1 – Cysteine/Lysine Residue(s) in Keap1 modified by OI as determ-ined by tandem mass spectrometry

4-OI Residue	Peptide Amino Acid Position	Peptide Sequence	-10logP	Enzyme	Digest Type
Cys23	22-31	S.KC(+242.15)PEGAGDAV.M	31.47	Elastase	In Gel
Cys151	144-152	A.SISVGEKC(+242.15)V.L	44.11	Elastase	In Gel
	146-152	I.SVGEKC(+242.15)V.L	30.95		
	144-153 A.SISVGEKC(+242.15)VL.H 30.25 145-152 S.ISVGEKC(+242.15)V.L 29.32				
Cys257	254-260	V.KYDC(+242.15)PQR.R	35.44	Elastase	In Gel
	255-260	K.YDC(+242.15)PQR.R	40.13	Trypsin	In Gel
	255-260	K.YDC(+242.15)PQR.R	41.08	Trypsin	In Solution
Cys273	273-279	R.C(+242.15)HALTPR.F	35.93	Trypsin	In Gel
	273-279	R.C(+242.15)HALTPR.F	38.65	Trypsin	In Solution
Cys288	282-293	L.QTQLQKC(+242.15)EILQA.D	41.70	Elastase	In Gel
	282-290	L.QTQLQKC(+242.15)EI.L	36.70		
	284-293	T.QLQKC(+242.15)EILQA.D	33.47		
	280-296	R.FLQTQLQKC(+242.15)EILQADAR.C	55.81	Trypsin	In Gel
	288-296	K.C(+242.15)EILQADAR.C	50.84		
	288-296	K.C(+242.15)EILQADAR.C	48.80	Trypsin	In Solution
Cys297	294-304	A.DARC(+242.15)KDYLVQI.F	37.15	Elastase	In Gel
K615	602-615	R.SGVGVAVTMEPCRK(+242.15).Q	37.59	Trypsin	In Gel
	602-615	R.SGVGVAVTM(+15.99)EPCRK(+242.15).Q	36.40		

Extended Data Table 1. Cysteine/Lysine Residue(s) in Keap1 modified by OI as determined by tandem mass spectrometry

Table 2 - Cysteine residues modified by itaconate identified using tandem mass spectrometry

LPS-treated BMDMs

Protein	Alkylated residue	Peptide amino acid position	Peptide sequence	X score	Ppm
Plsl	Cys111	97-123	KEGIC(+4.98)AIGGTSEQSSVGTQHSYSEEEK	5.998	-2.22
Acon	Cys385	378-395	VGLIGSC(+4.98)TNSSYEDMGR	4.212	4.17
Ldha	Cys84	82-90	DYC(4.98)VTANSK	3.474	-2.91
Anxa1	Cys189	186-204	GDRC(4.98)QDLSVNQDLADTDAR	3.514	-0.48
Ifi5b	Cys317	310-320	QMIEVPNC(+4.98)ITR	2.412	-4.16
Ipyr2	Cys156, 157	153-171	STDC(4.98)C(+4.98)GDNDPIDVCEIGSK	4.664	22.60
Ef2	Cys41	33-42	STLTDSLVC(+4.98)K	3.677	-1.41
Thio	Cys73	73-81	C(+4.98)MPTFQFYK	2.422	-2.22

OI-treated BMDMs

Protein	Alkylated residue	Peptide amino acid position	Peptide sequence	X score	Ppm
Gilt	Cys69	61-73	VSLYYESLC(+4.98)GACR	4.677	3.40
Fgd6	Cys1004	9996-1005	NVALLDEQC(+4.98)K	3.759	-7.98
Olfr644	Cys306	305-313	FC(+4.98)KILLGNK	3.155	-2.10
Ldha	Cys84	82-90	DYC(+4.98)VTANSK	2.832	3.88
Padi6	Cys553	553-558	C(+4.98)ISLNR	2.446	-18.58
Ubr4	Cys4241	4237-4244	LIASC(+4.98)HWK	2.421	-7.45
Hmox2	Cys314	314-323	C(+4.98)PFYAAQPDK	2.279	2.89
Lhpp	Cys113	112-118	FC(+4.98)TNESQK	2.169	-11.64

Extended Data Table 2. Cysteine residues modified following treatment with LPS (100 ng/ml) for 24 h (**top**) or OI (250 μM) (**bottom**) for 4 h.